The Physics of Cosmic Acceleration

Robert R. Caldwell[1] and Marc Kamionkowski[2]

[1]Department of Physics and Astronomy, Dartmouth College, Hanover, New Hampshire 03755; email: robert.r.caldwell@dartmouth.edu

[2]Division of Physics, Mathematics, and Astronomy, California Institute of Technology, Pasadena, California 91125; email: kamion@caltech.edu

Annu. Rev. Nucl. Part. Sci. 2009. 59:397–429

First published online as a Review in Advance on June 23, 2009

The *Annual Review of Nuclear and Particle Science* is online at nucl.annualreviews.org

This article's doi: 10.1146/annurev-nucl-010709-151330

0163-8998/09/1123-0397$20.00

Key Words

cosmology, dark energy, particle theory, gravitational theory

Abstract

The discovery that the cosmic expansion is accelerating has been followed by an intense theoretical and experimental response in physics and astronomy. The discovery implies that our most basic notions about how gravity works are violated on cosmological distance scales. A simple fix is to introduce a cosmological constant into the field equations for general relativity. However, the extremely small value of the cosmological constant, relative to theoretical expectations, has led theorists to explore numerous alternative explanations that involve the introduction of an exotic negative-pressure fluid or a modification of general relativity. Here we review the evidence for cosmic acceleration. We then survey some of the theoretical attempts to account for it, including the cosmological constant, quintessence and its variants, mass-varying neutrinos, and modifications of general relativity. We discuss experimental and observational tests that may allow us to distinguish among some of the theoretical ideas that have been proposed.

Contents

1. INTRODUCTION

The cosmic-acceleration puzzle is among the most viscerally compelling problems in physics. Our deepest intuition about gravity—that all objects should be attracted to one another—simply does not apply at cosmological distance scales. Rather than slowing, as Newtonian gravity predicts, the relative velocities of distant galaxies are increasing. The implication is either that gravity behaves far differently than we had previously thought or that some mysterious fluid (dark energy) with exotic gravitational properties fills the universe. Either way, there is new physics beyond the four fundamental forces described by the Standard Model and general relativity (GR). Cosmic acceleration thus motivates a considerable fraction of current physical cosmology research, and it has become a major focus of particle- and string-theory efforts.

There had long been hints, stemming primarily from the disparity among the values $\Omega_m \simeq 0.1 - 0.3$ of the nonrelativistic mass density found by dynamical measurements and the theoretical preference for a flat universe, $\Omega_{\rm tot} = 1$, that there may be a cosmological constant. However, direct measurements with distant supernovae of a negative deceleration parameter provided the "shot heard 'round the world" (1, 2). The case for an accelerated expansion was dramatically bolstered in 2000 with the cosmic microwave background (CMB) discovery of a flat universe (3). A combination of observations, based on galaxy surveys, the Lyman-alpha forest, and baryon acoustic oscillations (BAO), but primarily on the CMB, now provide constraints to cosmological

Dark energy: a negative-pressure fluid comprising ~75% of the cosmic energy budget, postulated to account for the accelerated cosmic expansion

GR: general relativity

CMB: cosmic microwave background

BAO: baryon acoustic oscillations

PROBLEMS WITH THE COSMOLOGICAL CONSTANT

A cosmological constant with $\Lambda = 3\Omega_\Lambda H_0^2/c^2$ provides a phenomenological description of dark energy; it implies that the vacuum "weighs" something—that is, that the vacuum gravitates. However, there is no physical understanding for why empty space would act as a source for the gravitational field. The particle physics vacuum contributes an effective cosmological constant, but with an energy density many orders of magnitude larger than is observed. This gross mismatch between theory and observation—noted by both Pauli (5) and Zeldovich (6)—is one of the deepest physical enigmas of our time. In quantum field theory, renormalization allows us to reset the energy density of the vacuum to zero, and for many years it was generally assumed that some mechanism made this cancellation precise and stable. However, the discovery of cosmic acceleration suggests that the cosmological constant is (in the absence of quintessence or some alternative gravity explanation for cosmic acceleration) small, but nonzero, and this has now changed the character of the cosmological constant problem. If the observational trend continues to favor dark energy with w_Q consistent with -1, the challenge will be to explain why the cosmological constant is so small, yet nonzero.

parameters at a precision that was almost unimaginable a decade ago. The evidence for cosmic acceleration exists now at the $\geq$10-σ level (4). It can no longer be ignored.

The simplest solution involves no more than the addition of a cosmological constant Λ (with units of curvature, or length^{-2}) to Einstein's equation. But the value required to explain cosmic acceleration is, in units where $G = c = \hbar = 1$, of order 10^{-120}. This is not a problem in the classical world, but the quantum field theory expectation is that the cosmological constant should be of order unity, or possibly zero, should some symmetry or dynamical mechanism operate. The gravitational effects of a cosmological constant are equivalent to those of the virtual particles that continually pop in and out of existence in quantum field theory. Renormalization allows us to choose the zero point of this virtual-particle energy density, but doing so implies a cancellation of terms in the fundamental Lagrangian to one part in 10^{120}.

Dark energy theories dodge this question. The effects of a cosmological constant in Einstein's equation can also be reproduced precisely by a homogeneous fluid of energy density $\rho_\Lambda = \Lambda c^4/8\pi G$ and pressure $p_\Lambda = -\rho_\Lambda$. Dark energy theories postulate that the vacuum itself does not gravitate (by virtue of some unspecified symmetry or dynamical mechanism), but that the universe is filled with dark energy, an exotic negative-pressure fluid that provides the impetus for cosmic acceleration. Alternative gravity theories investigated in this connection propose that an accelerated expansion may simply be the vacuum solution of the theory. The aim of the vast observational/experimental dark energy effort is to determine the physics of cosmic acceleration. See the sidebar, Problems with the Cosmological Constant, for further discussion.

Although dark energy and/or alternative gravity theories preclude the need for a cosmological constant, those that have been developed so far require (as we discuss below) the introduction of unusually tiny parameters and/or finely tuned initial conditions. They also introduce a new question, the so-called coincidence problem: Why has the universe transitioned from deceleration to acceleration so recently? None of the current models answers this question fully, although some (e.g., the tracker field models discussed below) do address it.

Theorists may debate the relative merits of various cosmic-acceleration theories—cosmological constant, dark energy, alternative gravity, anthropic arguments, etc.—but it is ultimately up to experiment to decide which is correct. The most telling empirical quantity in this regard is the (effective) dark energy equation-of-state parameter $w_Q \equiv p_Q/\rho_Q$, where p_Q and ρ_Q are the dark energy pressure and energy density, respectively. The parameter w_Q can be determined from the

Equation-of-state parameter: the ratio of the homogeneous pressure to the energy density, denoted $w = p/\rho$

expansion history; i.e., by how the cosmic acceleration changes with time. If cosmic acceleration is due to a cosmological constant, then $w_Q = -1$, and the future expansion is de Sitter–like (i.e., exponentially expanding). In contrast, dark energy and alternative gravity theories predict $w_Q \neq -1$. Current constraints are $w_Q \simeq -1 \pm 0.1$. The precise value of w_Q (and its evolution with time) depends on the particular cosmic acceleration theory. There is no consensus on how far from -1 this value should be, but we can provide some classification of theoretical predictions. Of course, cosmic acceleration theories require new physics, and this new physics may also be probed experimentally in other ways, beyond merely the expansion history.

This review is intended primarily to survey some of the theoretical explanations, involving both dark energy and alternative gravity, for cosmic acceleration, and secondarily to highlight the observational and experimental tests that may be pursued to test the theories. We begin with some background and a summary of the observational evidence for cosmic acceleration. We then review models that explain cosmic acceleration by the introduction of a new exotic fluid and those that work by modifying gravity. We close with a brief review of some of the observational/experimental ways forward. References 7–9 complement this review by providing deeper analyses of observational approaches to dark energy, whereas others (10–12) provide more details about recent dynamical models for dark energy.

2. BACKGROUND AND EVIDENCE

2.1. The Friedmann–Robertson–Walker Cosmology

We begin by reviewing the essentials of the standard cosmological model. We refer the reader to Chapter 13 in Reference 13 for more details.

2.1.1. Kinematics. An isotropic and homogeneous expanding universe with spatial coordinates x_i is described by the Robertson–Walker metric,[1] $ds^2 = -dt^2 + a^2(t)[dr^2 + r^2(d\theta^2 + \sin^2\theta\, d\phi^2)]$. The scale factor $a(t)$ is a function of time t, where $a(t_0) = a_0$ at the present time t_0. Cosmologists use the redshift $z \equiv (a_0/a) - 1$ as a proxy for the age or scale factor. The redshift can be measured for distant sources; it is the fractional amount by which the wavelength of a photon has been stretched by the expansion between the time the photon is emitted and the time it is received.

The expansion rate $H \equiv \dot{a}/a$ is a function of time, with the value $H_0 \simeq 70$ km s^{-1} Mpc^{-1} (the Hubble constant) and where the dot denotes a derivative with respect to t. The deceleration parameter is then $q \equiv -(\ddot{a}/a)/H^2 = (1+z)H'/H - 1$, where the prime denotes a derivative with respect to z. The luminosity distance of an object of luminosity L at a redshift z is defined as $d_L \equiv (L/4\pi F)^{1/2}$, where F is the energy flux received from that object. The luminosity distance is given (in a flat universe) by

$$d_L(z) = (1+z)c\int_0^z \frac{dz'}{H(z')}. \qquad 1.$$

Thus, measurement of the apparent brightness of sources of known luminosity (standard candles) at a variety of redshifts z can be used to determine or constrain the expansion history.

The quantity $[H(z)(1+z)]^{-1}dz$ determines the time that evolves between redshifts z and $z + dz$; thus, it also determines the physical distance in this redshift interval and therefore the physical volume in a given redshift interval and angular aperture. Likewise, $a(t)$ [which can be derived from $H(z)$] determines the angular sizes of standard rods, objects of fixed physical sizes. The

[1]Given the observational evidence for negligible spatial curvature, we assume throughout a flat universe. This simplifies considerably many of the equations. The effects of nonzero curvature are discussed in Reference 14.

angular-diameter distance is defined as $d_A(z) \equiv l_{\rm prop}/\theta$, where $l_{\rm prop}$ is the proper size of an object and where θ is the angle it subtends on the sky. The angular-diameter distance is related to d_L through $d_A(z) = (1+z)^{-2} d_L(z)$. As discussed below, measurements of the volume and luminosity and angular-diameter distances can also be used to determine the expansion history.

The integral expression for $d_L(z)$ can be Taylor expanded about $z = 0$ to quadratic order as $H_0 d_L(z) = c\,z[1+(1/2)(1-q_0)z+\cdots]$. The term linear in z is the well-known Hubble law. [Spatial curvature affects $d_L(z)$ only at cubic or higher order (14).] In 1998, two groups independently used supernovae as standard candles to find better than 3-σ evidence for a negative value for q_0 (1, 2), the implications of which we explain in the following subsections.

2.1.2. Dynamics. The Friedmann equation,

$$H^2 = \left(\frac{\dot{a}}{a}\right)^2 = \frac{8\pi G}{3}\sum_i \rho_i, \qquad 2.$$

is the general-relativistic equation of motion for $a(t)$ for a flat universe filled with fluids i (e.g., nonrelativistic matter, radiation, and dark energy) of energy densities ρ_i. If the fluids have pressures p_i, then the change $d(\rho a^3)$ in the total energy ($\rho = \sum_i \rho_i$) per comoving volume is equal to the work $-pd(a^3)$, where $p = \sum_i p_i$ done by the fluid. This relation allows us to rewrite the Friedmann equation as

$$\frac{\ddot{a}}{a} = -\frac{4\pi G}{3}\sum_i (\rho_i + 3p_i). \qquad 3.$$

A nonrelativistic source has pressure $p = 0$, implying that $\ddot{a} < 0$. In other words, the relative velocities between any two galaxies should be decreasing, in agreement with our Newtonian intuition.

If we define equation-of-state parameters $w_i \equiv p_i/\rho_i$ (e.g., $w_m = 0$ for matter and $w_r = 1/3$ for radiation), then the second form (Equation 3) of the Friedmann equation can be written $q_0 = (1+3w_t)/2$, where $w_t \equiv p/\rho$ is the net equation-of-state parameter. Thus, if GR is correct, the observations require that the universe has $w_t < -1/3$. Thus, some dark energy, a negative-pressure fluid, is postulated to account for cosmic acceleration.

2.1.3. Expansion history. Although the original supernova measurements determined only q_0, future measurements will aim to determine the full functional dependence of $d_L(z)$ [or, equivalently, $H(z)$] over the redshift range $0 < z \leq$ few. [The cubic correction to $d_L(z)$ was first obtained observationally in 2004 (15).] If the universe consists today of nonrelativistic matter (baryons and dark matter; $w_m = 0$) with current energy density $\Omega_m \equiv \rho_m/\rho_c$ (in units of the critical density $\rho_c = 3H_0^2/8\pi G$) and some other exotic fluid with energy density $\Omega_Q = 1-\Omega_m$ and an equation-of-state parameter w_Q, then $H(z) = H_0[\Omega_m(1+z)^3 + (1-\Omega_m)(1+z)^{3(1+w_Q)}]^{1/2}$. In a flat universe, $\Omega_m + \Omega_Q = 1$, the deceleration parameter is then $q_0 = (1+3w_Q\Omega_Q)/2$. The cosmological constant is equivalent to a fluid with $w_Q = -1$; in this case, $q_0 = (3/2)\Omega_m - 1$.

Note, however, that there is no reason to expect w_Q to be constant (unless $w_Q = -1$ precisely); this assumption is the simplest parameterization of a time-varying dark energy density. In much of the current literature [including the Dark Energy Task Force Report (7)], the time evolution of w_Q is parameterized as $w_Q = w_0 + w_a(1-a/a_0)$. Generally, though, $w_Q(z)$ may be an arbitrary function of z; it is up to the dark energy theory (which we have not yet specified) to predict. **Figure 1** shows the expansion history $H(z)$, luminosity distance $d_L(z)$, and deceleration parameter $q(z)$ for four different models. The first three models are constant-w_Q models, and the fourth model is an alternative gravity model (DGP gravity), described in Section 7.1 below, with variable

DGP: Dvali–Gabadadze–Porrati

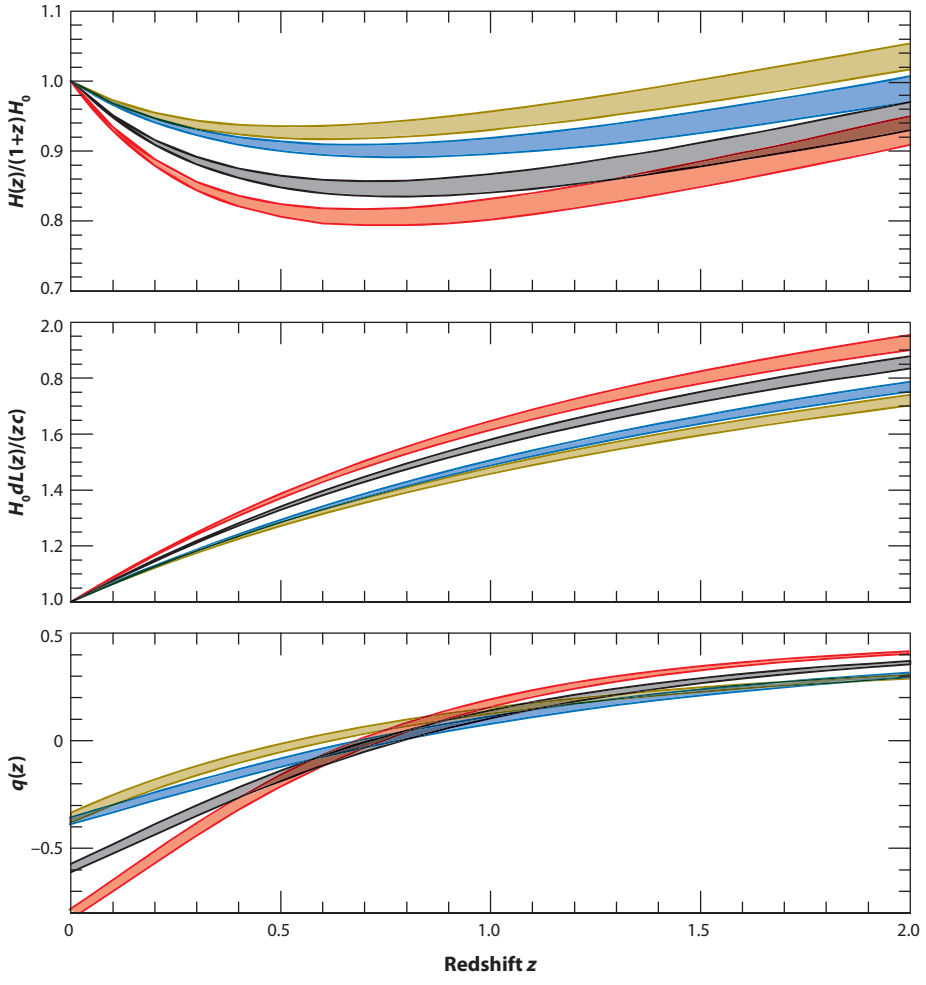

Figure 1

Examples of the expansion history $H(z)$, luminosity distance $d_L(z)$, and deceleration $q(z)$ are shown for several different dark energy models. The red, gray, and blue curves correspond to dark energy models with equation-of-state parameters $w_Q = -1.2$, -1, and -0.8, respectively. The brown curve is for a Dvali–Gabadadze–Porrati (DGP) alternative gravity model. All models have the same matter density and assume spatial flatness. The thickness of the curve areas indicates the uncertainties that arise from the current uncertainty in the nonrelativistic matter density Ω_m.

w_Q. Measurement of $w_Q(a)$ is the aim of observational efforts to probe the physics of cosmic acceleration.

2.1.4. Growth of structure. So far, we have assumed that the universe is perfectly homogeneous, but this is only an approximation; the fractional density perturbation $\delta_m(\vec{x}, t) \equiv [\rho_m(\vec{x}, t) - \bar{\rho}_m]/\bar{\rho}_m$, where $\bar{\rho}_m$ is the mean density, is not zero. At sufficiently early times, or when smoothed on sufficiently large scales, the fractional density perturbation is $\delta_m \ll 1$. In this linear regime, the density perturbation satisfies an evolution equation,

$$\ddot{\delta}_m + 2H\dot{\delta}_m - (3/2)\Omega_m H^2 \delta_m = 0. \qquad 4.$$

This equation has a growing-mode solution (as a function of z) $\delta_m(z) \propto D(z)$, and this evolution can be determined with large-scale structure measurements. In the standard cosmological model (i.e., $w_Q = -1$), the linear theory growth factor

$$D(z) \propto H(z)(5\Omega_m/2) \int_z^\infty (1+z)[H(z)]^{-3}\, dz.$$

However, this expression is invalid if $w_Q \neq -1$ (16), and $D(z)$ generally varies for different w_Q. Moreover, Equation 4 is derived assuming that the dark energy remains perfectly homogeneous. If dark energy clusters, there may be a source for this equation (i.e., the right-hand side may be nonzero), in which case $D(z)$ may be further affected. Alternative theories of gravity invoked to explain cosmic acceleration may predict a different $D(z)$, even for the same expansion history.

Quintessence: a dynamical dark energy; literally, the fifth element in the cosmic energy budget (in addition to radiation, baryons, neutrinos, and dark matter)

2.2. The Evidence

Evidence for accelerated expansion comes from the aforementioned direct measurements of $d_L(z)$ using Type Ia supernovae, which now suggest $q_0 \simeq -0.7 \pm 0.1$ (1-σ errors) (17). However, the case for accelerated expansion is dramatically bolstered by other observations. Chief among these is the CMB measurement of a flat universe (3), obtained by locating the first acoustic peak in the CMB power spectrum (18); this implies a total density $\Omega_m + \Omega_Q \simeq 1$ that is much greater than the matter density $\Omega_m \simeq 0.3$ indicated by dynamical measurements. Current CMB measurements alone are now sufficiently precise that they can determine a dark energy density $\Omega_Q = 0.742 \pm 0.030$ (for $w_Q = -1$ and a flat universe) (4), a measurement that is made still more precise with the addition of data from large-scale structure, the Lyman-alpha forest, BAO, the cluster abundance, and supernovae. In particular, supernova measurements provide a constraint (again, assuming $w_Q = -1$) $q_0 = (\Omega_m/2) - \Omega_Q \simeq -0.7$ that is nearly orthogonal to the CMB contour $\Omega_m + \Omega_Q \simeq 1$, and so CMB and supernovae together provide tight limits in the $\Omega_m - \Omega_Q$ plane. The consistency of a spatially flat universe with dark matter and a cosmological constant with a wealth of precise data has led to the adoption of a concordance model, our current standard cosmological model. Current values for the parameters of this model are provided in References 4 and 19.

The concordance model assumption $w_Q = -1$ can be tested quantitatively with the data. If the universe is flat, then the deceleration parameter is $q_0 = (1/2)(1 + 3w_Q\Omega_Q)$. If $q_0 < 0$, then $w_Q < -(1/3)(1 - \Omega_m)^{-1}$, or $w_Q \leq -0.5$ for $\Omega_m \leq 0.3$. The observed value $q_0 \simeq -0.7$ requires an even more negative pressure, with $w_Q \simeq -1$. The current constraints to the $\Omega_m - w_Q$ parameter space, assuming a constant w_Q and a flat universe, are shown in **Figure 2**. Very little is reliably known about the behavior of dark energy at $z \geq 1$, except that it does not appear to have played any significant role in cosmic evolution at earlier times. We discuss other probes of the expansion history in Section 9.

3. QUINTESSENCE

If the history of particle physics is any guide, then one can assume that the dark energy is due to a new field. For cosmology, the simplest field that can both provide the missing energy between the matter density and the critical density and drive cosmic acceleration is a scalar field. Such a field in this role is sometimes referred to as quintessence to help distinguish it from other fields or other forms of dark energy (20).

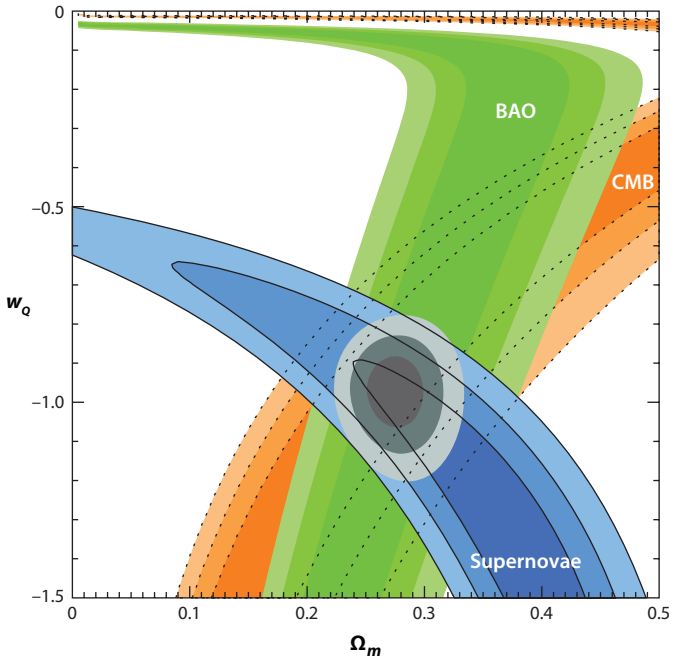

Figure 2

Shown are the 68.3%–, 95.4%–, and 99.7%–confidence level contours for w_Q and Ω_m, assuming a flat universe. The individual constraints from large-scale structure [using baryon acoustic oscillations (BAO)], the cosmic microwave background (CMB), and the Union Supernova data set are shown, as are the combined constraints. Reproduced from Reference 17 with permission.

3.1. Basic Equations

Here we review the basic equations of quintessence, beginning with those that describe the background evolution and its relation to the quintessence potential and then those that describe the evolution of perturbations to the quintessence field.

3.1.1. Background evolution. The formal description of quintessence begins with the action

$$S = \int d^4x\sqrt{-g}\left(\frac{R}{16\pi G} + \mathcal{L}_{SM} + \mathcal{L}_Q\right), \qquad 5.$$

where R is the Ricci scalar and where g is the determinant of the metric. Here, the quintessence Lagrangian is $\mathcal{L}_Q = -1/2(\nabla_\mu Q)(\nabla^\mu Q) - V(Q)$, and $\mathcal{L}_{SM}$ is the Lagrangian for Standard Model particles. The field obeys the Klein-Gordon equation, $\Box\, Q = V_{,Q}$, where $\Box$ is the d'Alembertian and $V_{,Q} \equiv \partial V/\partial Q$, and it carries stress-energy $T_{\mu\nu} = (\nabla_\mu Q)(\nabla_\nu Q) + g_{\mu\nu}\mathcal{L}_Q$. Note that we use metric signature $(-+++)$ and adopt the curvature conventions used in Reference 21.

The spatially homogeneous cosmic scalar is guided by the equation of motion, $\ddot{Q}+3H\dot{Q}+V_{,Q} = 0$, with energy density and pressure

$$\rho_Q = \frac{1}{2}\dot{Q}^2 + V(Q) \quad \text{and} \quad p_Q = \frac{1}{2}\dot{Q}^2 - V(Q). \qquad 6.$$

An equation-of-state parameter $w_Q < -1/3$ is obtained when $\dot{Q}^2 < V$. The mechanism for obtaining $\dot{Q}^2 \ll V$ is similar to the slow-roll mechanism in inflation (although not precisely the same, given that a fraction $\Omega_m \simeq 0.25$ of the current cosmological density is nonrelativistic matter).

We illustrate with the simple example of a potential $V(Q) = (1/2)m^2Q^2$. In the absence of the Hubble-friction term ($3H\dot{Q}$) in the scalar field equation of motion, the field simply oscillates in this quadratic potential. However, if $m \ll H$, then the Hubble friction overdamps the oscillator. In this case, $\ddot{Q} \ll H\dot{Q},\ V_{,Q}$, and $3H\dot{Q} \simeq -m^2Q$. The field then moves little over a Hubble time, and $\dot{Q}^2 \ll V$ is achieved. More generally, quintessence potentials are required to be very flat (i.e., to have effective masses $m_Q \equiv \sqrt{V_{,QQ}} \ll H$) to work.

3.1.2. Expansion history and the quintessence potential. A given quintessence potential determines the expansion history and vice versa. For example, if quintessence has an equation-of-state parameter $w(a)$ as a function of scale factor a, then the energy density can be reconstructed as

$$\rho_Q(a) = \Omega_Q\rho_c\ \exp\left(3\int_a^{a_0}[1+w(a)]\,d\ \ln\ a\right). \qquad 7.$$

The potential and field evolution for this equation-of-state parameter can then be reconstructed from

$$V(a) = \frac{1}{2}[1-w(a)]\rho(a),$$
$$Q(a) = \int d\tilde{a}\,\frac{\sqrt{1+w(\tilde{a})}}{\tilde{a}\,H(\tilde{a})}\sqrt{\rho(\tilde{a})}. \qquad 8.$$

The equivalence $w(a) \leftrightarrow V(Q[a])$ is valid provided that $\dot{Q} \neq 0$. For most quintessence models, in which the field evolves monotonically down a potential, this condition is satisfied.

3.1.3. Quintessence perturbations. If the quintessence field can vary in time, then it can generally vary in space. Linearized spatial fluctuations δQ of the quintessence field follow the evolution equation

$$\delta\ddot{Q} + 3H\delta\dot{Q} + \left(V_{,QQ} - \frac{1}{a^2}\nabla^2\right)\delta Q = \dot{\delta}_m\dot{Q}, \qquad 9.$$

where ∇^2 is the spatial Laplace operator in comoving coordinates and where δ_m is the nonrelativistic matter perturbation. Quintessence therefore responds to inhomogeneities in dark matter and baryons. Furthermore, the source term depends on $\dot{Q}$, so the closer w_Q is to -1, the weaker the driving term is. The nature of the response is determined by m_Q or by the quintessence Compton wavelength $\lambda_Q = m_Q^{-1}$. In the case of constant w_Q, there is a simplification that can be written as

$$V_{,QQ} = -\frac{3}{2}(1-w_Q)\left[\dot{H} - \frac{3}{2}(1+w_Q)H^2\right]. \qquad 10.$$

For a slowly varying equation-of-state parameter, $V_{,QQ} \propto H^2$ and $\lambda_Q \sim H^{-1}$. From the above equations, this means that fluctuations on scales smaller than the Hubble scale dissipate with sound speed equal to the speed of light because the coefficient of ∇^2/a^2 in Equation 9 is unity; hence, the field remains a smooth, nonclustering component. Any initial fluctuations in the quintessence field are damped out rapidly (22). In principle, perturbations to the quintessence field serve as a source for matter perturbations—i.e., they show up as a nonzero right-hand side to Equation 4—and thus affect the linear theory growth factor $D(z)$. However, the damping of small-scale quintessence perturbations implies that this is generically a small effect. On scales $\geq H^{-1}$, the field is gravitationally unstable. The growth of these long-wavelength perturbations to quintessence may leave an imprint on the large-angle CMB-anisotropy pattern, which we discuss in Section 3.4.

3.2. Representative Models

Embedding scalar field dark energy in a realistic extension of the Standard Model poses a number of challenges. A viable scenario generically requires an ultralight scalar ($m_Q \leq H \sim 10^{-42}$ GeV), with Planckian amplitude ($Q \sim 10^{19}$ GeV), that remains noninteracting with the Standard Model and therefore "dark" (23–26). A second challenge comes from the coincidence problem—Why is dark energy becoming dominant today? Ideally, the theory would have order-unity parameters at, say, the Planck scale, and the dark energy density today would be insensitive to the field's initial conditions. However, in existing models, the parameters of the potential are specially chosen so that quintessence provides acceleration today. Moreover, the scalar field generically requires finely tuned initial conditions if the field is to achieve the desired dynamics. Despite these difficulties, many models of quintessence have been proposed. Here we focus on a few representative models.

3.2.1. Cosmic axion. A cosmic axion, or pseudo-Nambu-Goldstone boson (PNGB), is one way to have a scalar of extremely low mass and to keep it dark. The first such models (27) considered a PNGB associated with a unification scale f mediating a breakdown of a global symmetry in a family of neutrinos at a scale $\mu \sim m_\nu^2/f$, thereby helping to explain the very light mass of the quintessence field. Models have been proposed employing string or M-theory moduli fields (28, 29) as well. The resulting scalar potential, $V = \mu^4(1 + \cos Q/f)$, remains stable against loop corrections [although not necessarily against quantum gravity effects (30, 31)], thereby protecting the mass μ. The shift symmetry, $Q \to Q + 2\pi f$, disables couplings to Standard Model fields that would otherwise spoil the "darkness." A viable scenario requires $\mu \simeq 0.002$ eV and $f \sim 10^{18}$ GeV (32–34). The cosmic evolution of the field is as follows: (*a*) The field has been frozen by Hubble friction through most of cosmic history; (*b*) as the Hubble friction relaxes, the field begins to slowly relax towards its ground state, as illustrated in **Figure 3**; and (*c*) in the future, the field will oscillate at the bottom of the potential, with its energy redshifting away like nonrelativistic matter. That the mass scales f and μ are derived from the energy scale of other physics alleviates some of the need to explain the coincidence problem. The initial position of Q on the potential directly determines the present-day properties of dark energy. However, the fine-tuning problem is eased because the PNGB potential is periodic; the range of starting values of Q that produces a viable scenario is a nonnegligible portion of the allowed range $Q \in [0, 2\pi f]$.

3.2.2. Tracker fields. Condensation of hidden-sector quark-antiquark pairs in a supersymmetric version of quantum chromodynamics has been shown to give rise to a pionlike scalar field with

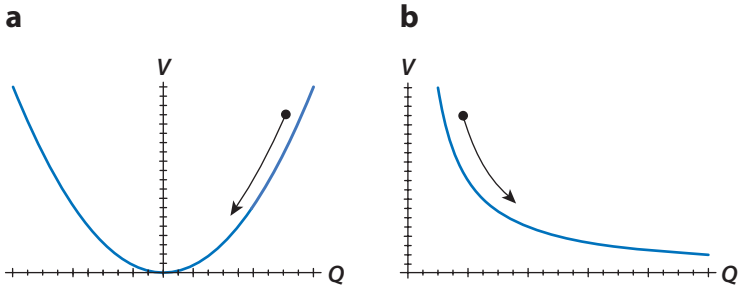

Figure 3

Two examples of potentials for the quintessence field. (*a*) One representative of a conventional massive scalar or pseudo-Nambu-Goldstone boson. The field is relaxing toward the local minimum. (*b*) One representative of vacuumless potentials such as the tracker. The field is evolving toward the global minimum.

an effective potential $V = M^4(Q/M_P)^{-n}$ with $n > 0$ (35, 36). The index n is determined by the number of fermion families and colors, and M is set by the cutoff scale. The cosmological dynamics of such a scalar are quite novel (37–40): For a broad range of initial conditions, the evolution of the field approaches, and then locks onto, a universal track with a negative equation-of-state parameter such that it inevitably dominates at late times. When the scalar field energy density is subdominant, its equation-of-state parameter is $w_Q \approx (nw_B - 2)/(n + 2)$, where w_B is the equation-of-state parameter of the dominant or background component. Thus, the field has been rolling down the potential for most of its history, as illustrated in **Figure 3**, but it is now beginning to slow. As the scalar field comes to dominate, its equation-of-state parameter grows more negative and goes asymptotically to $w_Q \to -1$ in the future. The universal track is uniquely determined by the mass M and index n, so there is a one-to-one relationship between Ω_Q and w_Q as a function of time. A viable model requires $0 < n < 1$ and $M \simeq 0.002$ eV. The broad insensitivity of the late-time behavior to the initial conditions is appealing—this model solves the abovementioned fine-tuning problem. Another feature of this model is that it helps to address the coincidence problem by allowing the dark energy density to track the matter/radiation density over long periods of cosmological history. Still, there is no explanation as to why the acceleration is happening now, as opposed to some later time.

3.2.3. Exponential potential. A scalar field with an exponential potential, $V = M^4 e^{-\lambda Q/m_{\rm Pl}}$, arises in a wide variety of extensions of Standard Model physics. In one particular case, the scalar field is the dilaton, a pionlike condensate of supersymmetric gaugino particles (36, 41). The dynamics of this model are as follows: (*a*) For $\lambda^2 > 3(1 + w_B)$ the scalar field energy density tracks the background fluid with $w_Q = w_B$, and (*b*) for $\lambda^2 < 2$, there are accelerating solutions (42). However, the scaling solutions do not satisfactorily convert into dark energy at late times; a viable model requires $\lambda^2 < 2$ and finely tuned initial conditions for Q and $\dot{Q}$. Phenomenological variations on this model have been explored in, for example, Reference 43. These models feature a local minimum in the exponentially decaying potential, where the field can relax and produce potential-dominated accelerating expansion.

3.2.4. Spintessence. A scalar field with internal degrees of freedom has been considered as a dark energy candidate; one particular example is termed spintessence (44), a complex field $Q = {\rm Re}^{i\Theta}$ spinning in a $U(1)$-symmetric potential $V = V(R)$. If the spin frequency is high enough, $\dot{\Theta} \gg H$, then it is rotation, rather than Hubble friction, that prevents the field from rolling immediately to its minimum. The equation-of-state parameter is $w \approx (RV' - V)/(RV' + V)$. Thus, a potential with shape $RV' < V/2$ can provide $w_Q < -\frac{1}{3}$. However, the field is generically unstable to the formation of Q-balls (nontopological solitons) (44, 45), rendering this solution to the dark energy problem unworkable. A gas of cold particles with an attractive interaction can also yield negative pressure (46), but in the relativistic regime required for cosmic acceleration, the theory resembles (47) spintessence. A related idea, termed oscillescence, is that a single real scalar field oscillates in a confining potential $V(Q) \propto |Q|^n$. This field acts like a fluid, with $w_Q = (n - 2)/(n + 2)$ (48), and thus gives $w_Q < -\frac{1}{3}$ for $n > 1$. Again, though, this model is unstable to small-scale perturbations (49).

3.2.5. k-Essence. Dark energy models with scalar degrees of freedom with noncanonical kinetic terms in the Lagrangian display novel dynamics. k-Essence defines a class of models with a Lagrangian $\mathcal{L}(Q, X)$ built from nonlinear functions of Q and $X \equiv -(1/2)(\nabla_\mu Q)(\nabla^\mu Q)$. The resulting stress-energy tensor is $T_{\mu\nu} = \mathcal{L}_{,X}(\nabla_\mu\phi)(\nabla_\nu\phi) + \mathcal{L}g_{\mu\nu}$, so the cosmic pressure is simply

Braneworld: scenario in which Standard Model fields are confined to a membrane in a higher-dimensional spacetime but gravity propagates everywhere

$p = \mathcal{L}$ and the energy density is $\rho = 2Xp_{,X} - p$. The motivation for these models is largely phenomenological, although in string-inspired models the scalar is identified with the dilaton or other moduli fields (50). Purely kinetic k-essence, with $\mathcal{L} = \mathcal{L}(X)$, behaves as a barotropic fluid (51). A k-essence counterpart to the potential-dominated tracker has $\mathcal{L} = f(\phi)(-X + X^2)$ with $f \propto \phi^{-n}$. For $0 < n < 2$, k-essence evolves with a constant equation-of-state parameter $w_Q = -1 + (n/2)(1 + w_B)$ until it comes to dominate the universe, whereupon $w_Q \to -1$ (52). Models with multiple attractor solutions, such that the field scales with an equation-of-state parameter $w_Q = 1/3$ during the radiation era, but then runs off to a de Sitter–like solution after the onset of matter domination, have been proposed as possible solutions of the coincidence problem (53). However, there is another aspect of k-essence that must be considered: The sound speed for the propagation of high-frequency perturbations is $v^2 = p_{,X}/\rho_{,X}$. The canonical scalar field has $v^2 = 1$. The k-essence models that predict $v^2 < 0$ can be eliminated because they are unstable to the growth of fluctuations. Density fluctuations in models with $0 < v^2 \ll 1$ can leave a strong imprint on the CMB and large-scale structure. The apparent violation of causality in models with $v^2 > 1$, including models that pass from scaling in the radiation era to a present-day accelerating solution (54), suggests that additional analysis is required to understand the phenomenology of these models (55).

3.2.6. Ghost condensate. Dark energy scalar field theories built from higher-order derivatives have also been studied. As an extension of k-essence, these models are also motivated by string field theory or braneworld scenarios and typically consist of a Lagrangian that is a nonlinear function of X, $\Box Q$, $(\nabla_\mu \nabla_\nu Q)(\nabla^\mu \nabla^\nu Q)$, etc. In certain cases, these higher-derivative terms can stabilize theories with a leading-order kinetic term of the wrong sign (hence, a ghost). One such case, a ghost condensate (56), has an equation-of-state parameter $w_Q = -1$ but carries fluctuations with a nonlinear dispersion relation $\omega^2 \propto k^4$. This fluid contributes to the overall inhomogeneous density field, yet the higher-derivative terms mean that its fluctuations are sourced by higher derivatives of the local gravitational fields. Generally, the additional dynamics resulting from the higher-derivative terms allow novel behavior such as $w_Q \leq -1$ with a stable but vanishing sound speed, $v^2 \to 0$ (57). Stable, nonrelativistic fluctuations contribute like a new species of dark matter inhomogeneties.

3.3. Thawing and Freezing Models

The equation-of-state parameter for dynamical dark energy is unlikely to be a constant. Using the cosmic axion and the tracker field as guides, we may identify two classes of quintessence models, thawing and freezing. Thawing models have a potential with a $V = 0$ minimum accessible within a finite range of Q. The field starts high up the potential, frozen by Hubble friction, with an equation-of-state parameter $w_Q = -1$. As the Hubble constant decays, the field begins to thaw and roll down toward $w_Q = 0$. Freezing models are said to be vacuumless, as the minimum is not accessible within a finite range of Q, although there are no barriers; the field rolls down the potential, but decelerates so that the equation-of-state parameter evolves towards $w_Q \to -1$. This ignores models with nonzero local minima of the potential, but these models are equivalent to a cosmological constant with massive scalar field excitations. The trajectories of thawing and freezing models occupy rather well-defined regions of the w_Q versus $dw_Q/d\ \ln a$ parameter plane (58), which are illustrated in **Figure 4**. [Plenty of models lie outside these regions (59, 60), although they tend to have metastable minima, e.g., a cosmological constant or noncanonical kinetic terms.] These regions can be used as a guide for assessing the sensitivity of methods to test for dynamical dark energy.

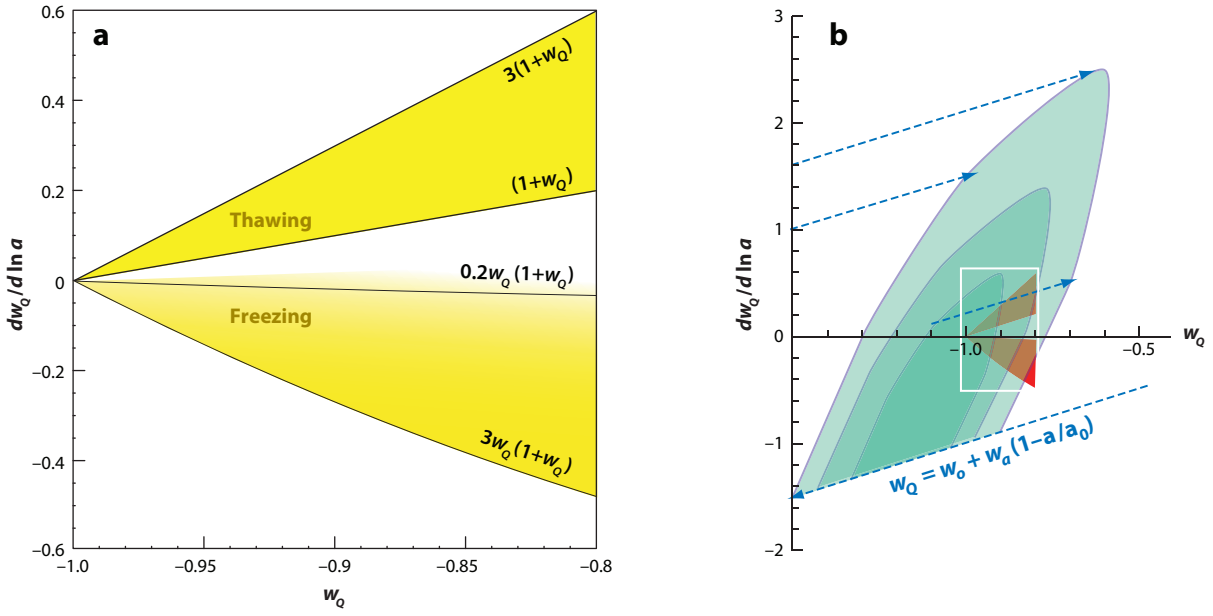

Figure 4

Shown is the w_Q versus $dw_Q/d\ \ln\ a$ parameter plane of dynamical dark energy models. (*a*) The likely range of thawing and freezing models. (*b*) The current 68.3%–, 95.4%–, and 99.7%–confidence level constraints on the dark energy parameterization $w_Q = w_0 + w_a(1 - a/a_0)$ (17) have been converted into the present-day values of w_Q, $dw_Q/d\ \ln\ a$. The dashed lines show the direction of evolution of models located at particular points on the 99.7%–confidence level boundary.

3.4. Observables of the Models

The dark energy observables are the energy density Ω_Q, equation-of-state parameters w_0 and w_a, and the growth factor $D(z)$, which is determined by the fluctuation sound speed v. The models described in this section predict some time evolution $a(t)$, which can then be recast in terms of w_0, w_a. The models also predict fluctuations of the dark energy density that propagate at a sound speed $v = 1$ for quintessence, or more generally $v \geq 0$ for k-essence. The dark energy density and equation-of-state parameter affect the expansion history $H(z)$. The growth rate of baryonic and dark matter perturbations, as well as the gravitational potentials sampled by CMB photons, are sensitive to the expansion history. Fluctuations in the dark energy, dependent upon the dark energy density, equation-of-state parameter, and sound speed, can leave an imprint on large-scale structure and the CMB. The impacts of these phenomena on the CMB power spectrum are illustrated in **Figure 5**. A further discussion of observational approaches is provided in Section 9.

4. MASS-VARYING NEUTRINOS

The coincidence between the mass scale $m_\Lambda \equiv \Lambda^{1/4} \sim 10^{-3}$ eV of the cosmological constant and that of neutrino masses motivates a solution that connects cosmic acceleration to neutrino physics. This idea was pursued in References 62 and 63 in the idea of mass-varying neutrinos (MaVaNs). Like quintessence, the theory introduces a slowly varying scalar field, dubbed the acceleron, whose value determines the neutrino mass m_ν. The increased energy density associated with larger m_ν affects the acceleron dynamics in such a way that the slow variation of the dark energy density can be achieved without an extremely flat scalar field potential.

MaVaN: mass-varying neutrino

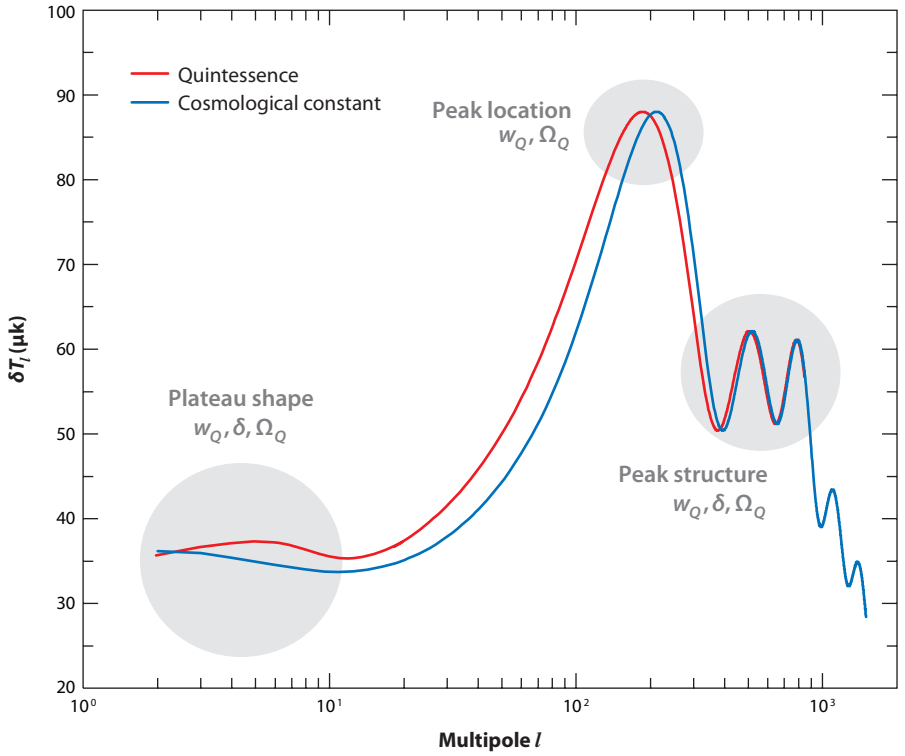

Figure 5

The effects of dynamical dark energy on the cosmic microwave background (CMB) temperature power spectrum are broadly illustrated. The dark energy, through its abundance and equation of state, indicated by Ω_Q and w_Q, influences the angular-diameter distance to last scattering, which sets the acoustic-peak multipole location. Similarly, dark energy influences the growth rate of perturbations, affecting the CMB anisotropies created at late times on large angular scales. Fluctuations in the dark energy, indicated by δ, also contribute to the anisotropy pattern. Dark energy can also influence the acoustic peak structure if it has a nonnegligible abundance at recombination (61).

More quantitatively, the energy density of the neutrino–dark energy fluid is $\rho_{\rm dark} = m_\nu n_\nu + \rho_a(m_\nu)$, where n_ν is the neutrino number density and where ρ_a is the acceleron density. For the sake of simplicity, the neutrinos are assumed to be nonrelativistic. The fields of the theory are designed so that the acceleron relaxes to the value that minimizes $\rho_{\rm dark}$, and the field value is thus fixed by the condition $(\partial\rho_{\rm dark}/\partial m_\nu) = n_\nu + (\partial\rho_a/\partial m_\nu) = 0$. Combining this with the energy-conservation equation $\dot\rho_{\rm dark} = -3H(\rho_{\rm dark} + p_{\rm dark})$, one finds that the dark sector equation-of-state parameter is

$$w \equiv \frac{p_{\rm dark}}{\rho_{\rm dark}} = -1 + \frac{m_\nu n_\nu}{m_\nu n_\nu + \rho_a}, \qquad 11.$$

which gives $w \simeq -1$.

Specific implementations of the theory may have testable consequences for neutrino-oscillation experiments (64). Unfortunately, however, the MaVaN idea suffers from a generic instability (65, 66) to the growth of perturbations that renders it unsuitable for explaining cosmic acceleration. The dark energy density at any given point is determined exclusively by the neutrino number density. The gradient-energy density in this model is too small to prevent the growth of spatial fluctuations. Thus, the sound speed is $c_s^2 = w < 0$, giving rise to a dynamical instability to the

rapid growth of perturbations to the MaVaN energy density. A similar instability arises generically in other models that similarly attempt to couple dark matter and dark energy (67, 68).

5. PHANTOM ENERGY

The simplest dark energy models (single-field models with canonical kinetic terms) have $w_Q \geq -1$. However, current data are consistent with $w_Q < -1$; for example, a recent analysis finds $-1.14 < w_Q < -0.88$ (95% CL) (19). What if the dark energy is phantom energy (69)? In other words, what if it has an equation-of-state parameter $w_Q < -1$? Generally, dark energy with $w_Q < -1$ fits to observational data with a slightly lower energy density Ω_Q than does dark energy with $w_Q > -1$. There are important differences, though, that stem from the fact that $w_Q < -1$ implies a violation of the null energy condition. This means the energy density grows, rather than decays, with time. In a phantom-dominated universe, the scale factor and expansion rate diverge in finite time, ripping apart everything—galaxies, stars, atoms—before the universe terminates in a "big rip" singularity (70, 71). For example, assuming the equation-of-state parameter maintains the constant value $w_Q = -1.1$, the end would arrive in ∼100 gigayears (Ga). Spacetime diagrams classifying the fate of the universe with different types of dark energy are given in Reference 72.

Theoretical models of phantom dark energy require exotic physics, such as a scalar field with negative kinetic energy or higher-derivative terms (69, 73). A quantum field with negative kinetic energy is unstable; even if it is dark, gravitational interactions—unless cut off at a sufficiently low energy scale (73, 74)—can catalyze a catastrophe. Curved-space quantum field–theory models of phantom energy are discussed in References 75 and 76. Quantum effects may strengthen a big rip or a sudden singularity (a singularity in which the scale factor remains finite but where its derivatives diverge) (77) when the spacetime-curvature radius shrinks to Planckian radius (78, 79). There are other mechanisms that could masquerade as phantom energy, such as novel photon (80) or dark matter interactions (81), as well as new gravitational phenomena (75). Although a canonical or k-essence scalar cannot cross the $w_Q = -1$ barrier (82–84), such evolution may be achieved in the presence of higher-derivative terms (85).

6. SCALAR-TENSOR AND $f(R)$ THEORIES

An alternative approach to cosmic acceleration is to change gravity. With quintessence, we assume that GR is correct but that the universe contains some exotic new substance that drives cosmic acceleration. Specifically, the left-hand side ($G_{\mu\nu}$) of Einstein's equation remains unaltered, but we introduce a new source $T_{\mu\nu}$ for the right-hand side. Here we alter GR, that is, replace the left-hand side of Einstein's equation, or change gravity even further.

6.1. Scalar-Tensor Theories

We begin by reviewing scalar-tensor theories, perhaps the most widely studied class of alternative gravity theories. A wide array of experimental tests of such theories have been investigated in detail (21). Scalar-tensor theories appear as low-energy limits of string theories, and other alternative gravity theories, such as $f(R)$ theories (discussed below), can be recast as scalar-tensor theories. They can be understood heuristically as models of gravity with a variable Newton's constant.

6.1.1. The action and field equations. In scalar-tensor theories, the Einstein–Hilbert action $S_{\rm EH} = (16\pi G)^{-1} \int d^4x\sqrt{-g}R$ for gravity is replaced by an action (see, e.g., Reference 86)

$$S = \int d^4x\sqrt{-g}\left[b(\lambda)R - \frac{1}{2}h(\lambda)g^{\mu\nu}(\partial_\mu\lambda)(\partial_\nu\lambda) - U(\lambda) + \mathcal{L}_M(g_{\mu\nu}, \psi_i)\right], \qquad 12.$$

where $\lambda(\vec{x}, t)$ is the eponymous scalar field; $\mathcal{L}(g_{\mu\nu}, \psi_i)$, the matter Lagrangian, is a function of the metric and matter fields ψ_i; and $b(\lambda)$, $h(\lambda)$, and $U(\lambda)$ are functions that determine the form of the scalar-tensor theory. The presence of a spatially varying field $b(\lambda)$ that multiplies the curvature R in Equation 12 implies that scalar-tensor theories are theories of gravity with a Newton's constant that depends on $b(\lambda)$. The other terms in the action are then kinetic- and potential-energy terms for the new field. Although Equation 12 suggests that three functions [$b(\lambda)$, $h(\lambda)$, and $U(\lambda)$] are required to specify the theory, we can redefine b to be the new field and then derive new functions $U(b)$ and $h(b)$.

Variation of the action with respect to the metric leads to the equation of motion (the generalization of Einstein's equation),

$$G_{\mu\nu} = b^{-1}(\lambda)\left[\frac{1}{2}T^{(M)}_{\mu\nu} + \frac{1}{2}T^{(\lambda)}_{\mu\nu} + \nabla_\mu\nabla_\nu b - g_{\mu\nu}\Box b\right], \qquad 13.$$

where $G_{\mu\nu}$ is the Einstein tensor, $T^{(M)}_{\mu\nu}$ is the stress tensor for matter, and

$$T^{(\lambda)}_{\mu\nu} = h(\lambda)(\nabla_\mu\lambda)(\nabla_\nu\lambda) - g_{\mu\nu}\left[\frac{1}{2}h(\lambda)g^{\rho\sigma}(\nabla_\rho\lambda)(\nabla_\sigma\lambda) + U(\lambda)\right] \qquad 14.$$

is the stress tensor for the scalar field. There is also an equation of motion,

$$h\Box\lambda + \frac{1}{2}h'g^{\mu\nu}(\nabla_\mu\lambda)(\nabla_\nu\lambda) - U' + b'R = 0, \qquad 15.$$

for the scalar field, where $' \equiv d/d\lambda$.

6.1.2. Friedmann equations. The equation of motion for the scale factor $a(t)$ in a spatially flat Robertson–Walker universe is

$$H^2 \equiv \left(\frac{\dot{a}}{a}\right)^2 = \frac{\rho}{6b} + \frac{h\dot{\lambda}^2}{6b} - H\frac{\dot{b}}{b} + \frac{U}{6b}, \qquad 16.$$

with scalar field equation of motion

$$\ddot{\lambda} + 3H\dot{\lambda} = 3\frac{b'}{h}\left(\dot{H} + 2H^2\right) - \frac{h'\dot{\lambda}^2}{2h} - \frac{1}{2}\frac{U'}{h}. \qquad 17.$$

Several things are made clear by these equations. First, there is considerable freedom in the choice of the functions $b(\lambda)$, $h(\lambda)$, and $U(\lambda)$, so it is difficult to make general statements about the validity of scalar-tensor theories. Second, specification of these functions alone does not determine the phenomenology; the initial conditions for the new scalar degree of freedom must also be specified.

Although the detailed Friedmann and scalar field equations are different, there are explanations for cosmic acceleration in these theories analogous to those in ordinary quintessence theories. For example, if $U(\lambda)$ is sufficiently shallow, there may be solutions to the equations of motion in which λ is displaced from the minimum of $U(\lambda)$ and rolls slowly. In this case, the time derivatives in the equations of motion will become negligible, the Friedmann equation becomes approximately $H^2 \simeq U/(6b) \simeq$ constant, and a roughly de Sitter expansion ensues. Given the additional terms in the Friedmann equation and scalar field equation of motion that depend on derivatives of b and h, the details may differ, and a wider range of behaviors may be possible. However, the form of the left-hand side of Equation 17 implies that the rolling of the scalar field generically slows with time; a general-relativistic cosmological behavior is consequently an attractor in many scalar-tensor theories (87).

6.1.3. Brans–Dicke theory and Solar System tests. The Brans–Dicke theory is defined by $b(\lambda) = \lambda/(16\pi G)$, $h(\lambda) = \omega/(8\pi\lambda G)$, and $U(\lambda) = 0$, where the Brans–Dicke parameter ω is a constant. Solution of the field equations in the Solar System gives rise to a parameterized post-Newtonian (PPN) parameter $\gamma = (\omega + 1)/(\omega + 2)$ for this theory. This parameter is measured in time-delay experiments in the Solar System to be $\gamma = 1 + (2.1 \pm 2.3) \times 10^{-5}$ (88), leading to a bound $\omega \geq 5 \times 10^4$. The generalization of this Solar System constraint to scalar-tensor theories with other choices of $b(\lambda)$, $h(\lambda)$, and $U(\lambda)$ depends on the specifics of those functions. Generally speaking, however, the bound applies as long as the curvature at the minimum of $U(\lambda)$ is sufficiently shallow so that the motion of λ within the Solar System is not restricted; below, this condition is quantified more precisely for $f(R)$ theories.

PPN: parameterized post-Newtonian

6.2. $f(R)$ Theories

One class of alternative gravity theories that has received considerable attention in recent years includes the $f(R)$ theories. We discuss these theories in the remainder of this section.

6.2.1. The action and field equations. The Einstein–Hilbert action of GR is replaced by an action (89)

$$S = \frac{1}{16\pi G}\int d^4x\sqrt{-g}\,f(R) + S_{\rm matter}, \qquad 18.$$

where $f(R)$ is a function whose form defines the theory. Such actions, which generalize the Einstein–Hilbert action, may arise as low-energy limits of string theory. Note that the G in this action is not necessarily the Newton's constant measured in terrestrial experiments.

The field equations are obtained by varying the action with respect to $g_{\mu\nu}$; the result is

$$f'(R)R_{\mu\nu} - \frac{1}{2}fg_{\mu\nu} - \nabla_\mu\nabla_\nu f'(R) + \Box f'(R)g_{\mu\nu} = 8\pi G T_{\mu\nu}. \qquad 19.$$

Taking the trace and setting $T_{\mu\nu} = 0$, we find a constant-curvature vacuum solution (i.e., a de Sitter spacetime) with scalar curvature R_0 and with $f'(R_0)R_0 = 2f(R_0)$.

6.2.2. $1/R$ gravity. For example, in $1/R$ gravity (90), we choose $f(R) = R - \mu^4/R$, where μ is a constant; this theory has a self-accelerating vacuum solution with $R = 12H^2 = \sqrt{3}\mu^2$. The field equation for this theory is

$$8\pi G T_{\mu\nu} = \left(1 + \frac{\mu^4}{R^2}\right)R_{\mu\nu} - \frac{1}{2}\left(1 - \frac{\mu^4}{R^2}\right)Rg_{\mu\nu} + \mu^4\left(g_{\mu\nu} - \nabla_{(\mu}\nabla_{\nu)}\right)R^{-2}. \qquad 20.$$

Some intuition about the model can be obtained from the trace,

$$\Box\frac{\mu^4}{R^2} - \frac{R}{3} + \frac{\mu^4}{R} = \frac{8\pi G T}{3}, \qquad 21.$$

where $T = g^{\mu\nu}T_{\mu\nu}$. For an effectively pressureless source (e.g., the Sun), $T = -\rho$, where ρ is the mass density. This trace should be compared with the general-relativistic Einstein equation trace, $R = 8\pi G\rho$. Note that (for constant R) the new equation is quadratic, rather than linear, in R, suggesting that there may be two different constant-curvature solutions for the same ρ. Given that $\mu^2 \sim H \ll G\rho$ in the Solar System, it is tempting to assume an approximate GR-like solution $R \simeq 8\pi G\rho$. However, this solution is violently unstable to small-wavelength perturbations (91), and it produces the wrong spacetime outside the Sun. The other solution, which has $R \simeq \mu^2$ everywhere throughout the Solar System (and which is very different from $R \sim G\rho$), is stable.

However, this solution predicts a PPN parameter $\gamma = 1/2$, which disagrees with experimental constraints (92, 93).

JBD: Jordan–Brans–Dicke

The other significant (and perhaps more important) difference between $1/R$ gravity and GR arises from the term $\Box\,(\mu^4/R^2)$ in Equation 21. In GR, the trace equation, $R = 8\pi G\rho$, is a constraint equation that determines R uniquely. However, in $1/R$ gravity, the scalar curvature R becomes a dynamical variable; in other words, there is a new scalar degree of freedom.

The original $1/R$ gravity theory is just one example of an $f(R)$ theory. Given the flexibility allowed in the choice of $f(R)$, it is unwise to draw general conclusions about $f(R)$ theories from $1/R$ gravity. Still, there are several lessons to be learned: (*a*) If the $f(R)$ theory is to explain cosmic acceleration, there are likely to be mass parameters comparable to H in the theory, (*b*) there is a scalar degree of freedom, dormant in GR, that comes to life in $f(R)$ theories, (*c*) Solar System constraints on the theory may be severe, (*d*) there may be more than one solution, for the same source, to the field equations, and (*e*) one of the solutions may be unstable to small-wavelength perturbations.

6.2.3. The equivalence between $f(R)$ and scalar-tensor theories. In the general case, the physics of $f(R)$ theories can be understood by noting that they are equivalent to scalar-tensor theories (92). Consider the following action for gravity with a scalar field λ:

$$S = \frac{1}{16\pi G}\int d^4x\sqrt{-g}\left[f(\lambda) + f'(\lambda)(R-\lambda)\right] + S_{\rm matter}. \qquad 22.$$

The λ equation of motion gives $\lambda = R$ if $f''(\lambda) \neq 0$, demonstrating the equivalence with Equation 18. Equation 22 is thus equivalent to the scalar-tensor action, Equation 12, if we identify $b(\lambda) = f'(\lambda)$, $U(\lambda) = -f(\lambda) + \lambda f'(\lambda)$, and $h(\lambda) = 0$. In other words, $f(R)$ theories are equivalent to scalar-tensor theories with vanishing kinetic terms. The absence of a kinetic term seems to suggest that the scalar degree of freedom remains dormant, but if we change to an Einstein-frame metric $g^E_{\mu\nu} = b'(\lambda)g_{\mu\nu}$ and canonical scalar field φ through $f'(\lambda) = \exp(\sqrt{16\pi G/3}\varphi)$, then the Jordan–Brans–Dicke–frame (JBD-frame) action (Equation 22) becomes, in the Einstein frame,

$$S = \int d^4x\sqrt{-g_E}\left[\frac{1}{16\pi G}R_E - \frac{1}{2}g_E^{\mu\nu}(\partial_\mu\varphi)(\partial_\nu\varphi) - V(\varphi)\right], \qquad 23.$$

where

$$V(\varphi) = \frac{\lambda(\varphi)f'(\lambda(\varphi)) - f(\lambda(\varphi))}{16\pi G[f'(\lambda(\varphi))]^2}. \qquad 24.$$

In this frame, the propagating scalar degree of freedom is apparent.

In the Einstein frame, scalar-tensor theories resemble GR with a canonical scalar field. The difference, though, is that the Einstein-frame metric g_E is not the metric whose geodesics determine particle orbits; it is the JBD-frame metric g. Thus, scalar-tensor theories in the Einstein frame resemble GR with an extra, nongeodesic force on the particle. These may also be generalized by "chameleon" theories (94), in which the scalar coupling to matter may differ for different matter fields. Viewed in the JBD frame, scalar-tensor theories are those in which there is a new propagating scalar degree of freedom, in addition to the usual two propagating tensorial degrees of freedom.

6.2.4. Friedmann equations. The Friedmann equations for $f(R)$ theory can now be obtained from Equation 16,

$$H^2 = \frac{1}{6}\frac{\rho}{f'(\lambda)} - H\frac{d}{dt}\ln f'(\lambda) + \frac{1}{6}\frac{\lambda f'(\lambda) - f(\lambda)}{f'(\lambda)}, \qquad 25.$$

and the scalar-field equation of motion, Equation 17, now provides the constraint $\lambda = 12H^2 + 6\dot{H}$. The self-accelerating solution, $H^2 = \lambda/12$, can be obtained by setting $\rho = 0$ and time derivatives equal to zero in these equations. Also, it is the scalar-field potential, $U(\lambda) = \lambda f'(\lambda) - f(\lambda)$, in the last term of Equation 25 that is driving the accelerated expansion.

6.2.5. Solar System constraints. The absence of a kinetic term for λ implies a Brans–Dicke parameter $\omega = 0$ and thus a PPN parameter $\gamma = 1/2$ for $f(R)$ gravity, generalizing the result for $1/R$ gravity. However, as discussed above, this Solar System constraint only applies if the function $U(\lambda)$ in the scalar-tensor theory is sufficiently close to flat that the scalar field can move freely in the Solar System. This is true if the following four conditions are satisfied (95): (*a*) $f(R)$ is analytic at $R = R_0$, where R_0 is the background value of R; (*b*) $f''(R_0) \neq 0$; (*c*) $|f'(R_0)/f''(R_0)|r_{SS}^2 \ll 1$, where where $r_{SS} \sim$ AU is the distance scale over which the Solar System tests are carried out; and (*d*) $|f'(R_0)/f''(R_0)| \ll R_0(r_\odot/GM_\odot)$. If these conditions are violated, then the linear theory analysis that concludes that $\gamma = 1/2$ breaks down. In this case, a fully nonlinear analysis is required to determine γ.

Theories can be constructed, by violating the fourth condition above, that exhibit a "chameleon" mechanism whereby the nonlinear solution satisfies Solar System constraints (96–98). These theories require the effective mass to be large in the Solar System and small in intergalactic space. The GR-like solution $R \simeq 8\pi G\rho$ inside the Sun matches the GR-like solution with $\rho \simeq \rho_{\rm MW}$ (where $\rho_{\rm MW}$ is the mass density in the Milky Way) outside the Sun, but within the Milky Way. That solution then transitions to the cosmological solution in intergalactic space. Functional forms for $f(R)$ that allow such behavior require several small parameters. Reference 99 provides a classification of such models. For example, an $f(R)$ that resembles a broken power law, in which $f(R) \propto R^n$ (with $n > 0$) as $R \to 0$ and $f(R) \propto a + b/R^n$ (where a and b are appropriately chosen constants), may work (96, 98). In these theories, the scalar field dynamics on cosmological scales become very stiff; in other words, the phenomenology of these theories is almost indistinguishable from those in which there is simply a cosmological constant (100).

These models also imply a tail-wags-the-dog effect whereby a change in the ambient density surrounding the Solar System, from interstellar medium densities to intergalactic medium densities, can change the results of PPN tests by five orders of magnitude. In some $f(R)$ theories, particularly those with a chameleon mechanism, the usual $1/r^2$-force law of gravity is modified. This seemingly trivial change may have profound implications for almost every area of astrophysics, from Solar System scales to the dynamics of galaxy clusters, few of which have yet to be thought through carefully.

6.2.6. Palatini formalism. In the usual formulation (the metric formalism) of GR, the Einstein–Hilbert action is varied with respect to the metric $g_{\mu\nu}$ to obtain Einstein's equations. However, an alternative approach, the Palatini formalism, is to vary the action with respect to both the connection $\Gamma^\rho_{\mu\nu}$ and the metric. If applied to the Einstein–Hilbert action, this approach results in the same gravitational field equations, and it also yields the standard relation between the metric and the connection. However, for a more general $f(R)$ action, the Palatini formalism gives rise to a different theory. Solutions to cosmic acceleration may also be obtained with the Palatini formalism (101), possibly without violating Solar System constraints. However, the Christoffel symbol is now evaluated using a different metric, $\tilde{g}_{\mu\nu} = f'(R)g_{\mu\nu}$, whereas particle trajectories still follow the geodesics of $g_{\mu\nu}$. Moreover, R is obtained from the algebraic relation $Rf'(R) - 2f(R) = 8\pi GT$ between the Ricci scalar and the trace of the stress-energy tensor. The gravitational implications depend sensitively on the source stress tensor. At the quantum level, these theories generally result

in new matter couplings that may have even more dire empirical consequences (102) in the form of violations of the equivalence principle (103).

7. BRANEWORLD GRAVITY AND RELATED IDEAS

The alternative gravity theories discussed above introduce a new scalar degree of freedom. Another possibility is to modify gravity by changing the dimensionality of space. In this section, we discuss such braneworld scenarios, as well as braneworld-inspired ideas. In braneworld scenarios, our $(3+1)-$d world is a subspace of a higher-dimensional spacetime. Unlike earlier extradimensional models (e.g., Kaluza–Klein theories), Standard Model fields may be restricted to lie on our brane, and gravitational fields may propagate in the extra dimensions (known as the bulk) as well.

7.1. Dvali–Gabadadze–Porrati Gravity

DGP (for Dvali–Gabadadze–Porrati) gravity (104, 105) postulates a $(4+1)$-dimensional universe in which the bulk of the five-dimensional spacetime is Minkowski space with an embedded $(3+1)$-dimensional brane (our universe) on which matter fields live.

7.1.1. The action. The gravitational action is

$$S_{(5)} = \int d^5x\sqrt{-g}\,\frac{R}{16\pi G^{(5)}} + \int d^4x\sqrt{-g^{(4)}}\left[\frac{R^{(4)}}{16\pi G} + L_{SM}\right], \qquad 26.$$

where $G^{(5)}$ is the five-dimensional gravitational constant (note that its dimensions are different from those of G), $g(R)$ is the five-dimensional metric determinant (Ricci scalar), and $g^{(4)}(R^{(4)})$ is the induced metric determinant (Ricci scalar) on the brane.

7.1.2. Heuristic picture. Before proceeding with the cosmological solution, consider DGP gravity in the weak field limit. If we take $g_{AB} = \eta_{AB} + h_{AB}$, where $|h_{AB}| \ll 1$, then the linearized field equations tell us that the four-dimensional metric components $h_{\mu\nu}$, wherein resides the nonrelativistic potential, have Fourier (p^μ) components,

$$h_{\mu\nu}(p) = \frac{8\pi G}{p^2 + 2(G/G^{(5)})p}\left[T_{\mu\nu}(p) - \frac{1}{3}\eta_{\mu\nu}T^\alpha_\alpha(p)\right], \qquad 27.$$

for a stress-energy source $T_{\mu\nu}$ on the brane. This suggests a crossover distance $r_0 = (1/2)(G^{(5)}/G)$. For Fourier modes $p \gg r_0^{-1}$, $h_{\mu\nu}(p) \propto p^{-2}$, implying the usual static gravitational potential $V(r) \propto r^{-1}$ for $r \ll r_0$. But for Fourier modes $p \ll r_0^{-1}$, $h_{\mu\nu}(p) \propto p^{-1}$, implying $V(r) \propto r^{-2}$ at larger distances. In other words, gravity is weaker at distances $r \geq r_0$.

The static gravitational potential in DGP gravity differs from that in fundamental theories with small extra dimensions. If there is an extra dimension curled up into a size $R_5 \sim$ mm, and if the graviton is free to propagate equally in our three spatial dimensions and this extra small dimension, then the gravitational force law steepens to r^{-3} at distances $\sim$mm. In DGP gravity, however, the extra dimension is large, not small, and there is an energy cost for the propagation of gravitons with wavelengths $\leq r_0$ into the bulk. At $r \leq r_0$, the gravitons are thus confined to the brane, and we have ordinary gravity. At $r \geq r_0$, the gravitons can escape into the bulk and the force law is that for a five-dimensional spacetime, as shown in **Figure 6**.

7.1.3. Cosmological solution. The action can be varied to obtain the field equations. The brane is then assumed to be filled with a homogeneous fluid of pressure p and energy density

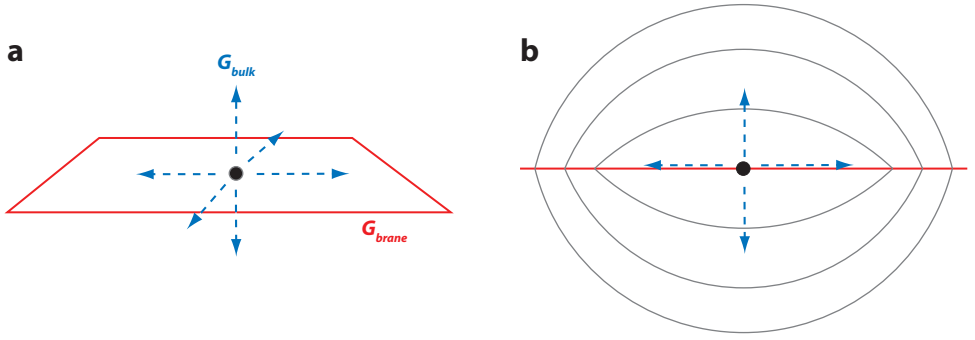

Figure 6

An illustration of the Dvali–Gabadadze–Porrati (DGP) mechanism. (*a*) Added to our $(3 + 1) - d$ spacetime (the brane) is an additional spatial dimension (the bulk). The presence of stress-energy on the brane provides an energy cost for the propagation of gravitons with wavelengths $<r_0$ into the bulk, thus making the gravitational force law $\propto r^{-2}$ at distances $r < r_0$ on the brane but $\propto r^{-3}$ at distances $r < r_0$. (*b*) Approximate equipotential curves for the gravitational field. Reproduced from Reference 106 with permission.

ρ (104, 107). Assuming a flat universe for the sake of simplicity, the cosmological metric takes the form $ds^2 = N^2(t, \xi)dt^2 - A^2(t, \xi)d\vec{x}^2 - B^2(t, \xi)d\xi^2$, where ξ is the coordinate for the fifth dimension. The (generalized) Einstein equations yield equations of motion for the metric variables $N(t, \xi)$, $A(t, \xi)$, and $B(t, \xi)$. The usual scale factor for our universe is then $a(t) = A(t, \xi = 0)$, and it satisfies an equation of motion (the DGP Friedmann equation)

$$H^2 \pm \frac{H}{r_0} = \frac{8\pi G}{3}\rho. \qquad 28.$$

There are two solutions for the expansion [cf., the discussion of $f(R)$ models, above]. If we take the minus sign in Equation 28, then at early times, when $H \gg r_0^{-1}$, we recover the usual Friedmann equation. But when H decreases, the new term kicks in, and $H \to r_0^{-1}$ at late times. In other words, the universe asymptotes at late times to a de Sitter phase. (The plus sign in Equation 28 results in an eternally decelerating universe.)

7.1.4. Solar System tests. Unlike quintessence models, which retain GR, DGP gravity is an alternative gravity theory, and it makes predictions for modified gravitational physics, beyond a modified expansion rate, and in particular for a modified spacetime in the Solar System. Superficially, at Solar System–distance scales DGP gravity resembles a theory with a gravitational scalar degree of freedom. This can be seen from the tensor structure, $T_{\mu\nu} - (1/3)\eta_{\mu\nu}T^{\alpha}_{\alpha}$, that acts as the source for the linearized gravitational field in Equation 27. This tensor structure resembles that in an $\omega = 0$ scalar-tensor theory and in massive gravity (the extra scalar being the longitudinal mode of the graviton), but it differs from the structure $T_{\mu\nu} - (1/2)\eta_{\mu\nu}T^{\alpha}_{\alpha}$ in GR. The extra scalar degree of freedom in DGP gravity may be understood as a fluctuation in the brane surface. The difference means that a relativistic particle (e.g., a photon) is affected differently by the same source, leading to a PPN parameter $\gamma = 1/2$, which again disagrees with measurements. This is a DGP equivalent of the van Dam–Veltman–Zakharov discontinuity (108, 109) that appears in massive gravity.

However, Equation 27 provides only the $(3 + 1)$–dimensional components of the field. The approximations that lead to this linearized equation involve a highly nonlinear metric perturbation in the bulk, even when the source is weak, thereby calling the derivation of Equation 27 into

question. A proper treatment involves a perturbative expansion not only in $h_{\mu\nu}$, but also in r/r_*, where $r_* = (r_g r_0^2)^{1/3}$ and where $r_g = 2GM/c^2$ is the Schwarzchild radius (110). The field equations for the spherically symmetric spacetime can then be solved perturbatively in three different distance regimes, with the following results: (*a*) The spacetime resembles that in GR, with fractional corrections $O((r/r_*)^{3/2})$, at small distances, $r \ll r_*$; (*b*) it resembles that in an $\omega = 0$ scalar-tensor theory (i.e., the static potential is still $\propto r^{-1}$, but light deflection is described by $\gamma = 1/2$) at distances $r_* \ll r \ll r_0$; and (*c*) it then falls off more steeply, as r^{-2}, at distances $r \gg r_0$.

For example, $r_* \simeq 150$ pc for the spacetime around the Sun. Thus, Solar System tests of gravity occur deep within the GR-like regime, and DGP gravity is thus consistent with these tests. Still, the spacetime is not precisely Schwarzchild; there are corrections $O((r/r_*)^{3/2})$. These corrections may be tested by future experiments (111), although the $r^{-3/2}$ dependence of the correction means that the theory cannot be parameterized with the usual PPN formalism.

Light-deflection experiments in the Solar System are unlikely to be constraining, as the fractional correction to the general-relativistic value for the deflection angle will be $\sim(r/r_*)^{3/2} \sim 10^{-11}$, whereas the smallest value probed is $\sim 10^{-4}$. However, measurements of perihelion advances may be more promising. DGP gravity leads to a correction, ~ 5 μas per year, to the perihelion advance of a planetary orbit (111). Unlike the general-relativistic perihelion-advance rate, which decreases for larger-r orbits, the DGP correction is r independent and can thus be distinguished from a general-relativistic correction (or from those that occur in the usual PPN expansion). Moreover, Solar System tests at large distances may be equally effective (or more effective) at testing DGP gravity as those at short distances. Thus, improved lunar laser ranging experiments may be sensitive to DGP gravity (112), as might BepiColombo and MESSENGER—European Space Agency and NASA satellites, respectively—to Mercury. However, probes of the outer Solar System, like Cassini, could also probe DGP gravity.

7.1.5. Expansion history. By rearranging Equation 28, we can rewrite the expansion history as $H(z) = (H_0/2)[1 - \Omega_m + \sqrt{(1-\Omega_m)^2 + 4\Omega_m(1+z)^3}]$. At $z \gg 1$, this approaches the standard form, $H(z) \simeq \sqrt{\Omega_m} H_0 (1+z)^{3/2}$, and $w_Q \to -1$ in the distant future, $z \to -1$. The deceleration parameter for this model is $q_0 = 3\Omega_m(1+\Omega_m)^{-1} - 1$, and thus there is a relation between q_0 and Ω_m. A value $\Omega_m = 0.274$ implies $q_0 = -0.355$, which is only marginally consistent with current data. A better fit to observations can be obtained by adding a cosmological constant or curvature (113) or in models based on other manifestations of braneworlds.

Figure 1 shows the expansion history, luminosity distance, and deceleration for the DGP model. If the expansion history can be measured with sufficient precision to distinguish this functional form from, e.g., a constant-w_Q model, then this may provide an avenue toward testing the model.

7.1.6. Growth of structure. The distance scales relevant for large-scale structure generally occur at $r \geq r_*$, where the behavior of DGP gravity differs from that of GR. The growth of linear density perturbations can be described in DGP gravity in terms of an effective Newton's constant, $G_{\rm eff} = G(1 + 3/\beta)$ (114), where $\beta = 1 - 2r_0 H\left[1 + \dot{H}/(3H^2)\right]$. The effects of this altered gravitational constant can be taken into account approximately by changing the last term in Equation 4; the factor $\Omega_m H^2$ that appears there arises from the Friedmann equation $\Omega_m H^2 = 8\pi G\rho/3$. The change in the linear theory growth factor $D(z)$ can be appreciable in these models; it is a $\sim 30\%$ correction at $z = 0$. This contrasts dramatically with quintessence models, which do not generally affect $D(z)$ significantly.

7.2. Related Ideas

There have been other attempts to modify gravity to account for cosmic acceleration that are inspired by DGP gravity or the massive gravity theories it resembles.

7.2.1. Degravitation. The idea of degravitation (115, 116) is to replace Einstein's equation, $G_{\mu\nu} = 8\pi G T_{\mu\nu}$, by $[1 + F(L^2\Box)]G_{\mu\nu} = 8\pi G T_{\mu\nu}$, where $F(x)$ is a monotonically decreasing filter function with the limits $F(x) \to 0$ for $x \to \infty$ and $F(x) \gg 1$ for $x \to 0$. Here, L is a distance scale (presumably $\sim H_0^{-1}$) at which the force of gravity weakens. Thus, Newton's constant acts as a high-pass filter; long-wavelength modes of the stress-energy tensor do not source the gravitational field. An analogous modification of electrodynamics is precisely equivalent to electrodynamics with a massive photon. Likewise, the structure of degravitation shares some similarities with massive gravity, although the mapping is not precise.

7.2.2. The fat graviton. The idea here (117) is to postulate that virtual gravitons with invariant masses at or above the millielectronvolt range simply do not propagate; the cosmological constant due to zero-point fluctuations conveyed by gravity is then observed. Such models can be constrained by considering cosmological gravitational lensing systems (118), as the angular deflection of photons in such systems implies momentum transfers (presumably carried by virtual gravitons) larger than this energy scale.

7.2.3. Modified Friedmann equations. Braneworld scenarios that generalize the DGP theory by allowing for a wider range of dynamics in the bulk can produce an effective expansion law $H^2 \propto \rho^n$ on the brane (119), and this has motivated phenomenological models of dark energy. One such example is the "Cardassian" model, whereby $H^2 = (8\pi G\rho/3) + B\rho^n$ (120); supernova and CMB distances suggest $n \leq 0.4$. An alternative parameterization of the effects of extra dimensions proposes $H^2 + (1 - \Omega_M)H_0^2(H/H_0)^\alpha = 8\pi G\rho/3$ (121). During the matter era, the equation-of-state parameter of the inferred dark energy is $w_{\rm eff} = -1 + \alpha/2$ until $z \sim 1$, and it asymptotes to $w_{\rm eff} \to -1$ in the future. Rough arguments suggest that $\alpha \leq 1$ is necessary for consistency with observations.

7.2.4. A phenomenological approach. The authors of References 122–124 posit the existence of a new gravitational theory that changes the amount of spacetime curvature produced per unit mass. The Friedmann equation is modified so that the matter-dominated expansion becomes progressively more de Sitter–like, mimicking the evolution under dynamical dark energy with equation-of-state parameter $w_Q \simeq -1$. Metric perturbations likewise respond differently to inhomogeneities in the matter and radiation, leading to a characteristic "gravitational slip" whereby the potential ψ appearing in the geodesic equation, $\ddot{\vec{M}} = -\vec{\nabla}\psi$, differs from the potential ϕ in the Poisson equation, $\nabla^2\phi = 4\pi G\delta\rho$. Scalar-tensor and $f(R)$ theories, braneworld scenarios, and DGP gravity, as well as massive gravity, all predict $\phi \neq \psi$ in the presence of nonrelativistic matter, in contrast to GR. This suggests a parameterized post-Friedmann description of modified gravity, whereby a new parameter, $\varpi \equiv \psi/\phi - 1$, characterizes the degree of departure from GR, in analogy to the post-Newtonian parameter γ. The imposed time and scale dependence of ϖ, along with two further assumptions—conservation of the radiation and matter stress-energy tensor and the absence of new gravitational effects mimicking a "dark fluid" momentum flux or velocity relative to the cosmic rest frame—are sufficient to complete the description of linearized metric perturbations. A $\varpi \neq 0$ affects the rate of growth of perturbations, the integrated Sachs–Wolfe

effect, and the weak gravitational lensing deflection angle. Hence, observations of the CMB and large-scale structure may be used to test for the consistency of GR on cosmological scales.

Landscape scenario: idea that string theory predicts a huge number of false vacua with different but closely spaced vacuum-energy densities

7.3. Comments

There are a number of theoretical questions that must be addressed if braneworld scenarios are to explain cosmic acceleration. The simplest DGP model is only marginally consistent with the observed cosmic acceleration; either some new exotic fluid or a more complicated implementation of the braneworld must be introduced to improve the agreement with the data. Braneworld scenarios introduce new small parameters, and they do not solve the coincidence problem. Moreover, we do not know whether the local perturbative solutions for the spherically symmetric DGP spacetime can be sewn together into a single global solution (125). There are also questions about the stability of the self-accelerating phase to the growth of small-scale fluctuations (126, 127). Still, braneworld scenarios and related ideas are worth further theoretical attention, as they connect cosmology to novel ideas from string and supergravity theories and provide a range of phenomenological consequences beyond the alteration of the expansion rate that they were introduced to explain.

8. THE LANDSCAPE SCENARIO

In this review, we have concentrated on theories of cosmic acceleration based on the introduction of new fields or modifications of gravity, both intended as alternatives to the simple postulate of a cosmological constant. But cosmic acceleration may simply be due to a cosmological constant. If so, then the physics of cosmic acceleration is just the physics of the cosmological constant. We have refrained from discussing theories of the cosmological constant (for reviews, see References 128 and 129), but we make an exception for the recently developed landscape scenario (130).

Like quintessence, the landscape scenario allows for a range of possible values for the vacuum energy. Unlike quintessence, these possibilities are arranged in a so-called discretuum, rather than a continuum, of values. The spacing between these values is comparable to the observed value of the cosmological constant. To understand the idea, recall that the electromagnetic field $F_{\mu\nu}$ is a two-form field (an antisymmetric rank-two tensor) sourced by a charge e that follows some worldline. In $1+1$ dimensions (or equivalently, between two parallel plates), the electric field and its energy density are constant. Quantization of the electron charge e implies that both the field and energy density are quantized, the latter taking on values $\rho \propto n^2 e^2$, where n is an integer.

Similarly, a four-form field $F_{\mu\nu\rho\sigma}$ in $3+1$ spatial dimensions is sourced by coupling to an electrically charged membrane (a 3-brane), and in string theory, there are also analogs of magnetic charges (5-branes). Quantization conditions, analogous to the Dirac quantization condition in electromagnetism, then require that the field and the associated energy density take on discrete values: $\rho = (1/2) n^2 q^2 m_{\rm Pl}^4$ (130–132).

Suppose now that there is a "bare" cosmological constant $\lambda = O(m_{\rm Pl}^2)$, which, for the sake of argument, may be negative. Then the effective cosmological constant Λ can take on values $\Lambda = \lambda + 4\pi n^2 q^2 m_{\rm Pl}^2$. There is thus an infinite range of possible values of Λ. The requirement that there be one that is $\Lambda \lesssim 10^{-120} m_{\rm Pl}^2$ requires $q \lesssim 10^{-120} \lambda^{1/2} m_{\rm Pl}^{-1}$; in other words, there is still a fine-tuning problem. Put another way, if $q \sim 1$, then the closest that $n^2 q^2$ gets to $-\lambda/m_{\rm Pl}^2$ is ~ 1, or in other words, the density of states is constant in n.

However, in string theory, there may be a large number j of four-form fields; for instance, a typical value may be $J \simeq 100 - 500$. If so, then the cosmological constant takes on values $\Lambda = \lambda + 4\pi \sum_i n_i^2 q_i^2 m_{\rm Pl}^2$. Taking all $q_i = q$, for the sake of argument, each combination $\{n_1, n_2, \ldots, n_J\}$ describes a different vacuum with a contribution $\lambda_n \equiv 4\pi q^2 m_{\rm Pl}^2 \sum_i n_i^2$ to the vacuum-energy

density. The number of states with $n^2 \equiv \sum_i n_i^2$ in the range $n^2 \to n^2 + dn^2$ is $(dN/dn^2)dn^2$, where $(dN/dn^2) = (2\pi)^{J/2} n^{J-2} [2\Gamma(J/2)]^{-1}$, the density of states, is proportional to the area of a J-sphere of radius n. The typical spacing between states is thus $4\pi q^2 m_{\rm Pl}^2 \Delta(n^2)$, where $\Delta(n^2) = (dN/dn^2)^{-1}$. If we assume $\lambda_n \simeq m_{\rm Pl}^2$, then $n^2 \simeq (4\pi q^2)^{-1}$. Taking $4\pi q^2 \simeq 0.01$, we find $\Delta(n^2) \simeq 10^{-120}$ for $J \simeq 200$. Thus, the presence of many four-form fields allows for far more closely spaced levels in the cosmological constant discretuum and thus explains how a value $10^{-120}\, m_{\rm Pl}^2$ may arise in string theory.

9. THE OBSERVATIONAL WAY FORWARD

9.1. The Expansion History

The evidence for dark energy or modified gravity comes from measurements that probe the expansion history of the universe, and extensions of these measurements provide perhaps the most promising avenues for further empirical inquiry. Current data show that the cosmic expansion is accelerating, and they constrain the dark energy density to within a few percent. If we assume that the equation-of-state parameter w_Q is constant, then it is constrained to be within 12% of -1 (at a 95% confidence level) (19).

The question is whether cosmic acceleration is due solely to a cosmological constant, or whether there is something more interesting going on. Thus, a number of avenues are being pursued to measure w_Q more precisely to determine whether it can be shown to be different from -1. These probes have recently been reviewed thoroughly by the Dark Energy Task Force (DETF) (7) and elsewhere (8, 9), so we simply summarize them here. In principle, the expansion history can be determined with a variety of cosmological observations (e.g., quasar-lensing statistics, cluster properties, the Lyman-alpha forest, the Alcock–Paczynski test, direct measurements of the age of the universe, etc.). However, the DETF focused upon supernovae, galaxy-cluster abundances, BAO, and weak gravitational lensing, reflecting a rough consensus in the community that these four approaches currently provide the most promising avenues. We caution, however, that there may still be room for new ideas. Either way, it is generally agreed that given systematic errors inherent in any particular technique, several complementary methods will be required to provide cross-checks.

9.1.1. Supernovae. Supernovae have played a crucial role in establishing cosmic acceleration, and they are likely to provide even more precise constraints on the expansion history in the future. To date, the supernovae used in such studies are Type Ia, explosions powered by the thermonuclear detonation of a white dwarf when its mass exceeds the Chandrasekhar limit. These explosions can be distinguished from those produced by other mechanisms (e.g., Type II supernovae, powered by iron-core collapse in supergiants) from the details of their spectra and light curves. The fact that the star ignites very rapidly after exceeding the Chandrasekhar limit implies that Type Ia supernovae should be good standard candles. Thus, their observed brightness provides the luminosity distance $d_L(z)$. Measurements support this simple notion, and details of the spectra and light curves can be used to correct for relatively small changes in the supernova luminosities.

Supernova searches will be particularly valuable if they can reach redshifts $z \sim 1$, where the effects of different w_Q values become most dramatic (see **Figure 1**). Progress with supernovae will require greater reduction in systematic errors, better theoretical understanding of supernovae and evolution effects, and greater statistics. Both ground-based and space-based supernova searches can be used to determine the expansion history. However, for redshifts $z \sim 1$, the principal optical supernova emission (as well as the characteristic silicon absorption feature) gets shifted to the infrared, which is obscured by the atmosphere, and this provides (much of) the case for a space-based observatory.

9.1.2. Baryon acoustic oscillations. In recent years, BAO have become increasingly attractive as a possibility for determining the expansion history. The acoustic oscillations seen in the CMB power spectrum are due to oscillations in the photon-baryon fluid at the surface of last scatter. The dark matter is decoupled and does not participate in these oscillations. However, because baryons contribute a nonnegligible fraction of the nonrelativistic-matter density, oscillations in the baryon-photon fluid imprint as small oscillations in the matter power spectrum at late times (133, 134). These oscillations have now been detected in galaxy surveys (135). The physical wave number at which these oscillations occur is well understood from linear perturbation theory, and so they provide a standard ruler. Thus, BAO measure the angular diameter distance $d_A(z) = (1+z)^{-2} d_L(z)$. Measurement of clustering along the line of sight may also provide information on the expansion history $H(z)$. Issues with BAO include nonlinear evolution of the acoustic peaks in the matter power spectrum and systematic and astrophysical effects (136) that could mimic features in the power spectrum.

9.1.3. Cluster abundances. Galaxy clusters are the largest gravitationally bound objects in the universe. The spatial density of clusters in the universe can be determined from models of structure formation. The observed number of clusters depends on the spatial density as well as on the volume per unit solid angle on the sky and per unit redshift interval (137). This volume depends on the quantity $[H(z)(1+z)]^{-1}$, so clusters measure the expansion history $H(z)$.

The theories predict the cluster abundance as a function of the cluster mass. The trick, then, is to obtain the cluster mass from the cluster observables—namely, the luminosity and temperature of the X-ray emission, the Sunyaev–Zeldovich effect (138), cluster dynamics, and/or the effects of weak gravitational lensing by the cluster on background galaxies. There is now a large industry that amalgamates theory, simulations, and multiwavelength cluster observations in an effort to develop a reliable cluster-mass indicator.

9.1.4. Weak lensing. Weak gravitational lensing by large-scale density fluctuations along the line of sight to distant galaxies can distort the images of those galaxies (139). Large-distance correlations in the mass thereby induce long-distance correlations in the observed ellipticities of the distant galaxies. Measurements of these ellipticity correlations can thus be used to determine the power spectrum of the mass as a function of angular wave number. If the power spectrum is already known (e.g., from the CMB) as a function of the physical wave number, then the observed amplitude determines the physical wave number corresponding to an angular wave number. Thus, weak lensing measures the angular diameter distance $d_A(z)$. Weak lensing probes the gravitational potential and thus the total mass, unlike galaxy surveys, which use luminous galaxies to trace the mass distribution. The challenge with weak lensing is to understand the subtle experimental effects that might mimic weak lensing–induced ellipticity correlations. There may also be intrinsic alignments of the galaxies (140) that could resemble a weak lensing signal.

9.1.5. Other probes of the expansion history. There may be other ways to measure the expansion history. If the ages of stellar populations can be obtained from their spectra at a variety of redshifts, then the expansion rate dz/dt may be obtained directly (141). There may be other luminous standard candles; for example, the gravitational wave signal from supermassive black hole binaries (142) may provide a new method to determine luminosity distance if a suitable measure of redshift can be obtained from an optical counterpart. It has also recently been suggested that by comparing the biases and redshift-space distortions for two different galaxy populations, constraints to $D(z)$ and $H(z)$ may be obtained (143) in a way that is limited ultimately by the number of galaxies, rather than the number of Fourier modes in the density field.

9.2. Growth of Structure

The growth rate of density inhomogeneities [i.e., the linear theory growth factor $D(z)$] depends on the cosmic expansion rate. Moreover, different theories that predict the same background cosmic evolution may lead to different rates of perturbation growth. For example, DGP theories are expected to have a significant effect on $D(z)$, and above we discussed a phenomenological approach (parameterized post-Friedmann) to the growth of perturbations in alternative gravity theories. Of the four avenues discussed above, clusters, BAO, and weak lensing may also provide measurements of $D(z)$ in addition to measurements of $H(z)$.

9.3. Lorentz Violation and Other Tests

The new physics implied by cosmic acceleration, gravitational or otherwise, may have other observable/experimental consequences apart from its effect on cosmic expansion. For example, we have discussed Solar System tests of alternative gravity theories for cosmic acceleration and the differing effects of various models on the growth of large-scale structure.

Tests of Lorentz violation provide another avenue. The rest frame of the CMB provides us with a preferred frame in the universe. Because a cosmological constant has the same density in every inertial frame, it can manifest no effects of Lorentz violation. If, however, $w \neq -1$, due to either dark energy or modified gravity, and if that new physics is somehow coupled nongravitationally to ordinary matter, then the preferred cosmological frame may show up in tests of Lorentz violation. Typically, however, we expect these violations to be extremely small by laboratory standards. First of all, dark energy fields must be exceedingly weakly coupled to Standard Model particles if they are to remain dark. Moreover, the timescale for evolution of these fields is the Hubble time, far longer than laboratory timescales.

Cosmological observations may allow for the experimental timescale to be comparable to the Hubble time. For example, Carroll (23) pointed out that if quintessence couples to the pseudoscalar of electromagnetism, there will be a uniform rotation of the linear polarization of photons propagating over cosmological distances. This could be probed by looking for a mean misalignment between the linear polarization of cosmological radio sources with the position angles of their images. It can also be tested by looking for the parity-violating polarization correlations it produces in the CMB polarization (144).

In addition to these and laboratory tests of Lorentz violation, preferred-frame effects in gravitational physics may also arise if the quintessence field couples in some nontrivial way (145). Eötvös-like experiments may also be used to search for couplings of ordinary matter to the quintessence field. If cosmic acceleration is due to a scalar-tensor theory, then the variable Newton's constant implied by the theory may suggest that other fundamental constants vary with time (146).

It is easy to speculate how various dark energy theories may give rise to Lorentz violation, preferred-frame effects, or variation of fundamental constants. But in the absence of any clear front-runner theories, it is much more difficult to say which, if any of these, will be more constraining.

10. CONCLUSIONS

The nature of cosmic acceleration is an intriguing puzzle. Occam's razor suggests that the phenomenon may be explained simply by a cosmological constant. This may be an acceptable phenomenological explanation, but it would be more satisfying to have a physical explanation for the observed value of Λ. The unexpectedly small value inferred for Λ leads us to suspect that the apparent cosmological constant may be the false-vacuum energy associated with the displacement of

some field from its minimum and/or that there may be new gravitational physics beyond Einstein's GR. Plenty of interesting ideas for dark energy and alternative gravity have been conjectured, but there is no clear front runner. The models are all awaiting new, corroborating, or contraindicating evidence.

Some scientists have argued that no new physics is required, that nonlinear behavior in GR may exhibit subtleties that allow for an accelerated expansion. For example, the authors of Reference 147 proposed that superhorizon perturbations may induce accelerated expansion in our observable Hubble patch. This idea has been disproved (148–150), but it has not yet been disproved that subhorizon nonlinearities may explain the observations. Alternatively, it has been suggested that the luminosity-distance-redshift data can be explained if we reside at the center of a gigaparsec-scale void in an otherwise Einstein–de Sitter universe. But such a radially inhomogeneous, anti-Copernican scenario conflicts with other observations (151, 152). Any future proposals that attempt to dispense with new physics must explain the vast catalog of phenomena already explained by the standard cosmological model.

In principle, new theories of gravitation can work. However, it has proved to be more difficult than may have originally been anticipated to alter gravity to explain cosmic acceleration without violating Solar System constraints. The scalar-tensor or $f(R)$ theories that do succeed seem contrived, and/or they manifest themselves in a way that is virtually indistinguishable from a cosmological constant. Braneworld scenarios introduce the possibility of interesting gravitational physics in the Solar System and in large-scale structure, but the simplest models must be ornamented with additional ingredients to work. Generally, alternative gravity theories that alter the long-range $1/r^2$ force law may have profound implications for a variety of astrophysical systems, few of which have been explored carefully.

The simplest paradigm, quintessence, does not suffer from instabilities, and it can be viewed as an effective theory for more complicated models. Quintessence models do require small parameters and/or finely tuned initial conditions, and they do not address the coincidence problem. Still, the resemblance of some quintessence fields to both fundamental or composite scalars appearing in existing models of physics beyond the Standard Model allow us to hope that new particle discoveries, at the Large Hadron Collider or beyond, may provide the clues to connect this dark energy field to the world of luminous matter.

The next step for cosmological studies should be to determine whether w_Q departs significantly from -1. If it does, then the step beyond that will be to measure its time evolution w_a. The w_0–w_a measurement may then tell us something qualitative about dark energy dynamics (e.g., thawing or freezing potentials). If so, we can proceed from there.

SUMMARY POINTS

1. The cosmic expansion is observed to be accelerating.
2. The physical mechanism responsible for the cosmic acceleration is unknown. Interpreting the observational and experimental evidence in the context of Einstein's GR, the causative agent appears to be an exotic fluid, referred to as dark energy, with negative pressure.
3. A cosmological constant is equivalent to such a fluid with a constant energy density. However, the value of this energy density, in units where $G = c = \hbar = 1$ is 10^{-120}, and there is no good explanation for the smallness of this value.

4. Quintessence postulates that the dark energy is associated with a scalar field that has been displaced from the minimum of its potential. Such theories generally predict an equation-of-state parameter for dark energy of $w_Q \neq -1$, as opposed to the cosmological constant, which has $w_Q = -1$.
5. Other explanations for cosmic acceleration propose that a new gravitational theory supplants Einstein's GR on cosmological scales. However, new theories are tightly constrained by precision tests of gravitation within the Solar System.
6. In the absence of a clear front-runner theory, most efforts are directed toward refining measurements of the cosmic expansion history to determine more precisely the value of w_Q.
7. A combination of cosmological observations is expected to gain the most traction toward an understanding of the physics of cosmic acceleration. The most attention has focused on four techniques: supernovae, BAO, cluster abundances, and weak lensing.

FUTURE ISSUES

1. Will future results from the Large Hadron Collider have any impact on dark energy theory? Could the discovery of supersymmetry, a nonstandard Higgs, or large extra dimensions change the way we think about dark energy?
2. Will string theory make a robust prediction for the cosmological constant, or perhaps otherwise explain the physics of cosmic acceleration?
3. Can an elegant and consistent modification to GR explain cosmic acceleration while still satisfying Solar System constraints?
4. Will there be NASA and ESA satellite missions to study dark energy within 5–10 years?
5. How much will ground-based observations and experiments refine our knowledge of the physics of cosmic acceleration?
6. Will new connections between other probes of new physics (e.g., dark matter searches, gravitational waves, probes of gravity on submillimeter scales, Lorentz invariance violation) and dark energy be found?
7. Relevant future observations will include measurements of the cosmic expansion history with greater accuracy and studies of the growth of large-scale structure. More work must be done to determine the best avenue forward.

DISCLOSURE STATEMENT

The authors are not aware of any memberships, affiliations, funding, or financial holdings that might be perceived as affecting the objectivity of this review.

ACKNOWLEDGMENTS

We thank S. Carroll, A. Erickcek, J. Frieman, T. Smith, and A. Weinstein for useful comments on an earlier draft. This work was supported at Caltech by Department of Energy grant

DE-FG03-92-ER40701 and the Gordon and Betty Moore Foundation and at Dartmouth by National Science Foundation grant AST-0349213.

LITERATURE CITED

1. **Perlmutter S, et al. (Supernova Cosmol. Proj. Collab.) *Astrophys. J.* 517:565 (1999)**
2. **Riess AG, et al. (Supernova Search Team Collab.) *Astron. J.* 116:1009 (1998)**
3. de Bernardis P, et al. (Boomerang Collab.) *Nature* 404:955 (2000)
4. Dunkley J, et al. (WMAP Collab.) *Astrophys. J. Suppl.* 180:306 (2009)
5. Straumann N. *Space Sci. Rev.* doi:10.1007/s11214-009-9486-9. hist-ph/0810.2213 (2008)
6. Zeldovich YB. *Sov. Phys. Usp.* 11:381 (1968)
7. **Albrecht A, et al. astro-ph/0609591 (2006)**
8. **Frieman J, Turner M, Huterer D. *Annu. Rev. Astron. Astrophys.* 46:385 (2008)**
9. Linder EV. *Rep. Prog. Phys.* 71:056901 (2008)
10. Peebles PJE, Ratra B. *Rev. Mod. Phys.* 75:559 (2003)
11. Padmanabhan T. *Phys. Rep.* 380:235 (2003)
12. **Copeland EJ, Sami M, Tsujikawa S. *Int. J. Mod. Phys. D* 15:1753 (2006)**
13. Peebles PJE. *Principles of Physical Cosmology*. Princeton, NJ: Princeton Univ. Press (1993)
14. Caldwell RR, Kamionkowski M. *JCAP* 0409:009 (2004)
15. Riess AG, et al. (Supernova Search Team Collab.) *Astrophys. J.* 607:665 (2004)
16. Wang LM, Steinhardt PJ. *Astrophys. J.* 508:483 (1998)
17. Kowalski M, et al. *Astrophys. J.* 686:749 (2008)
18. Kamionkowski M, Spergel DN, Sugiyama N. *Astrophys. J.* 426:L57 (1994)
19. Komatsu E, et al. (WMAP Collab.) *Astrophys. J. Suppl.* 180:330 (2008)
20. Caldwell RR, Dave R, Steinhardt PJ. *Phys. Rev. Lett.* 80:1582 (1998)
21. Will CM. *Theory and Experiment in Gravitational Physics*. Cambridge, UK: Cambridge Univ. Press (1993)
22. Dave R, Caldwell RR, Steinhardt PJ. *Phys. Rev. D* 66:023516 (2002)
23. **Carroll SM. *Phys. Rev. Lett.* 81:3067 (1998)**
24. Kolda CF, Lyth DH. *Phys. Lett. B* 458:197 (1999)
25. Peccei RD. *Proc. Int. Symp. Sources Detect. Dark Matter Universe (DM 2000), 4th, Marina del Rey, Calif.*, p. 98. Berlin: Springer (2000)
26. Chung DJH, Everett LL, Riotto A. *Phys. Lett. B* 556:61 (2003)
27. Frieman JA, Hill CT, Stebbins A, Waga I. *Phys. Rev. Lett.* 75:2077 (1995)
28. Choi K. *Phys. Rev. D* 62:043509 (2000)
29. Kim JE, Nilles HP. *Phys. Lett. B* 553:1 (2003)
30. Kamionkowski M, March-Russell J. *Phys. Lett. B* 282:137 (1992)
31. Holman R, et al. *Phys. Lett. B* 282:132 (1992)
32. Coble K, Dodelson S, Frieman JA. *Phys. Rev. D* 55:1851 (1997)
33. Dutta K, Sorbo L. *Phys. Rev. D* 75:063514 (2007)
34. Abrahamse A, Albrecht A, Barnard M, Bozek B. *Phys. Rev. D* 77:103503 (2008)
35. Affleck I, Dine M, Seiberg N. *Nucl. Phys. B* 241:493 (1984)
36. Binetruy P. *Phys. Rev. D* 60:063502 (1999)
37. Peebles PJE, Ratra B. *Astrophys. J.* 325:L17 (1988)
38. Ratra B, Peebles PJE. *Phys. Rev. D* 37:3406 (1988)
39. Zlatev I, Wang LM, Steinhardt PJ. *Phys. Rev. Lett.* 82:896 (1999)
40. Steinhardt PJ, Wang LM, Zlatev I. *Phys. Rev. D* 59:123504 (1999)
41. Wetterich C. *Astron. Astrophys.* 301:321 (1995)
42. Copeland EJ, Liddle AR, Wands D. *Phys. Rev. D* 57:4686 (1998)
43. Albrecht A, Skordis C. *Phys. Rev. Lett.* 84:2076 (2000)
44. Boyle LA, Caldwell RR, Kamionkowski M. *Phys. Lett. B* 545:17 (2002)
45. Kasuya S. *Phys. Lett. B* 515:121 (2001)
46. Nishiyama M, Morita MA, Morikawa M. *Proc. XXXIXth Rencontres Moriond*, vol. 143. astro-ph/0403571 (2004)

1–2. First reports of direct evidence, from supernova measurements of the luminosity-distance-redshift relation, for an accelerated cosmic expansion.

7–8. Provide the most up-to-date and detailed reviews of observational probes of the expansion history.

12. Comprehensive and detailed review of dynamical models of dark energy.

23. Provides a cogent explanation of the difficulties in building a dark cosmic scalar field in a realistic model of particle physics.

47. Fukuyama T, Morikawa M. *Prog. Theor. Phys.* 115:1047 (2005)
48. Turner MS. *Phys. Rev. D* 28:1243 (1983)
49. Johnson MC, Kamionkowski M. *Phys. Rev. D* 78:063010 (2008)
50. Armendariz-Picon C, Damour T, Mukhanov VF. *Phys. Lett. B* 458:209 (1999)
51. Scherrer RJ. *Phys. Rev. Lett.* 93:011301 (2004)
52. Chiba T, Okabe T, Yamaguchi M. *Phys. Rev. D* 62:023511 (2000)
53. Armendariz-Picon C, Mukhanov VF, Steinhardt PJ. *Phys. Rev. Lett.* 85:4438 (2000)
54. Bonvin C, Caprini C, Durrer R. *Phys. Rev. Lett.* 97:081303 (2006)
55. Babichev E, Mukhanov V, Vikman A. *JHEP* 0802:101 (2008)
56. Arkani-Hamed N, Cheng HC, Luty MA, Mukohyama S. *JHEP* 0405:074 (2004)
57. Creminelli P, D'Amico G, Norena J, Vernizzi F. *JCAP* 0902:018 (2008)
58. Caldwell RR, Linder EV. *Phys. Rev. Lett.* 95:141301 (2005)
59. Huterer D, Peiris HV. *Phys. Rev. D* 75:083503 (2007)
60. Crittenden R, Majerotto E, Piazza F. *Phys. Rev. Lett.* 98:251301 (2007)
61. Caldwell RR, et al. *Astrophys. J.* 591:L75 (2003)
62. Fardon R, Nelson AE, Weiner N. *JCAP* 0410:005 (2004)
63. Peccei RD. *Phys. Rev. D* 71:023527 (2005)
64. Kaplan DB, Nelson AE, Weiner N. *Phys. Rev. Lett.* 93:091801 (2004)
65. Afshordi N, Zaldarriaga M, Kohri K. *Phys. Rev. D* 72:065024 (2005)
66. Brookfield AW, van de Bruck C, Mota DF, Tocchini-Valentini D. *Phys. Rev. D* 73:083515 (2006); Erratum. *Phys. Rev. D* 76:049901 (2007)
67. Anderson GW, Carroll SM. *Proc. COSMO-97: 1st Int. Workshop Part. Phys. Early Universe*, *Ambleside*, *Eng.*, p. 227. Singapore: World Sci. (1997)
68. Bean R, Flanagan EE, Trodden M. *Phys. Rev. D* 78:023009 (2008)
69. Caldwell RR. *Phys. Lett. B* 545:23 (2002)
70. Caldwell RR, Kamionkowski M, Weinberg NN. *Phys. Rev. Lett.* 91:071301 (2003)
71. McInnes B. *JHEP* 0208:029 (2002)
72. Chiba T, Takahashi R, Sugiyama N. *Class. Quant. Grav.* 22:3745 (2005)
73. Carroll SM, Hoffman M, Trodden M. *Phys. Rev. D* 68:023509 (2003)
74. Cline JM, Jeon S, Moore GD. *Phys. Rev. D* 70:043543 (2004)
75. Parker L, Raval A. *Phys. Rev. Lett.* 86:749 (2001)
76. Onemli VK, Woodard RP. *Phys. Rev. D* 70:107301 (2004)
77. Barrow JD. *Class. Quant. Grav.* 21:L79 (2004)
78. Calderon H, Hiscock WA. *Class. Quant. Grav.* 22:L23 (2005)
79. Barrow JD, Batista AB, Fabris JC, Houndjo S. *Phys. Rev. D* 78:123508 (2008)
80. Csaki C, Kaloper N, Terning J. *Ann. Phys.* 317:410 (2005)
81. Huey G, Wandelt BD. *Phys. Rev. D* 74:023519 (2006)
82. Vikman A. *Phys. Rev. D* 71:023515 (2005)
83. Hu W. *Phys. Rev. D* 71:047301 (2005)
84. Caldwell RR, Doran M. *Phys. Rev. D* 72:043527 (2005)
85. Li MZ, Feng B, Zhang XM. *JCAP* 0512:002 (2005)
86. Carroll SM. *Spacetime and Geometry: An Introduction to General Relativity.* San Francisco: Addison-Wesley (2004)
87. Damour T, Nordtvedt K. *Phys. Rev. D* 48:3436 (1993)
88. Bertotti B, Iess L, Tortora P. *Nature* 425:374 (2003)
89. Capozziello S, Carloni S, Troisi A. *Recent Res. Dev. Astron. Astrophys.* 1:625 (2003)
90. Carroll SM, Duvvuri V, Trodden M, Turner MS. *Phys. Rev. D* 70:043528 (2004)
91. Dolgov AD, Kawasaki M. *Phys. Lett. B* 573:1 (2003)
92. Chiba T. *Phys. Lett. B* 575:1 (2003)
93. Erickcek AL, Smith TL, Kamionkowski M. *Phys. Rev. D* 74:121501 (2006)
94. Khoury J, Weltman A. *Phys. Rev. D* 69:044026 (2004)
95. Chiba T, Smith TL, Erickcek AL. *Phys. Rev. D* 75:124014 (2007)
96. Starobinsky AA. *JETP Lett.* 86:157 (2007)

97. Faulkner T, Tegmark M, Bunn EF, Mao Y. *Phys. Rev. D* 76:063505 (2007)
98. Hu W, Sawicki I. *Phys. Rev. D* 76:064004 (2007)
99. Amendola L, Gannouji R, Polarski D, Tsujikawa S. *Phys. Rev. D* 75:083504 (2007)
100. Appleby SA, Battye RA. *Phys. Lett. B* 654:7 (2007)
101. Vollick DN. *Phys. Rev. D* 68:063510 (2003)
102. Flanagan EE. *Phys. Rev. Lett.* 92:071101 (2004)
103. Olmo GJ. *Phys. Rev. D* 72:083505 (2005)
104. Binetruy P, Deffayet C, Langlois D. *Nucl. Phys. B* 565:269 (2000)
105. Dvali GR, Gabadadze G, Porrati M. *Phys. Lett. B* 485:208 (2000)
106. Lue A. *Phys. Rep.* 423:1 (2006)
107. Deffayet C. *Phys. Lett. B* 502:199 (2001)
108. van Dam H, Veltman MJG. *Nucl. Phys. B* 22:397 (1970)
109. Zakharov VI. *JETP Lett.* 12:312 (1970)
110. Gruzinov A. *N. Astron.* 10:311 (2005)
111. Lue A, Starkman G. *Phys. Rev. D* 67:064002 (2003)
112. Dvali G, Gruzinov A, Zaldarriaga M. *Phys. Rev. D* 68:024012 (2003)
113. Deffayet C, et al. *Phys. Rev. D* 66:024019 (2002)
114. Lue A, Scoccimarro R, Starkman GD. *Phys. Rev. D* 69:124015 (2004)
115. Arkani-Hamed N, Dimopoulos S, Dvali G, Gabadadze G. hep-th/0209227 (2002)
116. Dvali G, Hofmann S, Khoury J. *Phys. Rev. D* 76:084006 (2007)
117. Sundrum R. *Phys. Rev. D* 69:044014 (2004)
118. Caldwell RR, Grin D. *Phys. Rev. Lett.* 100:031301 (2008)
119. Sahni V, Shtanov Y. *JCAP* 0311:014 (2003)
120. Freese K, Lewis M. *Phys. Lett. B* 540:1 (2002)
121. Dvali G, Turner MS. astro-ph/0301510 (2003)
122. Bertschinger E. *Astrophys. J.* 648:797 (2006)
123. Caldwell R, Cooray A, Melchiorri A. *Phys. Rev. D* 76:023507 (2007)
124. Hu W, Sawicki I. *Phys. Rev. D* 76:104043 (2007)
125. Damour T, Kogan II, Papazoglou A. *Phys. Rev. D* 67:064009 (2003)
126. Luty MA, Porrati M, Rattazzi R. *JHEP* 0309:029 (2003)
127. Gregory R. *Prog. Theor. Phys. Suppl.* 172:71 (2008)
128. Weinberg S. *Rev. Mod. Phys.* 61:1 (1989)
129. Carroll SM. *Living Rev. Rel.* 4:1 (2001)
130. Bousso R, Polchinski J. *JHEP* 0006:006 (2000)
131. Abbott LF. *Phys. Lett. B* 150:427 (1985)
132. Brown JD, Teitelboim C. *Phys. Lett. B* 195:177 (1987)
133. Eisenstein DJ, Hu W, Silk J, Szalay AS. *Astrophys. J.* 494:L1 (1998)
134. Seo HJ, Eisenstein DJ. *Astrophys. J.* 598:720 (2003)
135. Eisenstein DJ, et al. (SDSS Collab.) *Astrophys. J.* 633:560 (2005)
136. Pritchard JR, Furlanetto SR, Kamionkowski M. *MNRAS* 374:159 (2007)
137. Haiman Z, Mohr JJ, Holder GP. *Astrophys. J.* 553:545 (2000)
138. Carlstrom JE, Holder GP, Reese ED. *Annu. Rev. Astron. Astrophys.* 40:643 (2002)
139. Refregier A. *Annu. Rev. Astron. Astrophys.* 41:645 (2003)
140. Catelan P, Kamionkowski M, Blandford RD. *MNRAS* 320:7 (2001)
141. Jimenez R, Loeb A. *Astrophys. J.* 573:37 (2002)
142. Holz DE, Hughes SA. *Astrophys. J.* 629:15 (2005)
143. McDonald P, Seljak U. astro-ph/0810.0323 (2008)
144. Lue A, Wang LM, Kamionkowski M. *Phys. Rev. Lett.* 83:1506 (1999)
145. Graesser ML, Jenkins A, Wise MB. *Phys. Lett. B* 613:5 (2005)
146. Uzan JP. *Rev. Mod. Phys.* 75:403 (2003)
147. Kolb EW, Matarrese S, Notari A, Riotto A. hep-th/0503117 (2005)
148. Hirata CM, Seljak U. *Phys. Rev. D* 72:083501 (2005)
149. Geshnizjani G, Chung DJH, Afshordi N. *Phys. Rev. D* 72:023517 (2005)
150. Flanagan EE. *Phys. Rev. D* 71:103521 (2005)
151. Goodman J. *Phys. Rev. D* 52:1821 (1995)
152. Caldwell RR, Stebbins A. *Phys. Rev. Lett.* 100:191302 (2008)

106. Clear and detailed recent review of DGP gravity and cosmology.

128. Classic review on the cosmological constant.

RELATED RESOURCES

1. Uzan, JP. *Gen. Relativ. Grav.* 39:307 (2007)
2. Durrer R, Maartens R. astro-ph/0811.4132 (2008)
3. Caldwell RR. *Phys. World* 17:37. **http://physicsworld.com/cws/article/print/19419** (2004)
4. Nobbenhuis S. *Found. Phys.* 36:613 (2006)

Annual Review of Nuclear and Particle Science

Volume 59, 2009

Contents

Indexes

Errata

An online log of corrections to *Annual Review of Nuclear and Particle Science* articles may be found at http://nucl.annualreviews.org/errata.shtml